A COMPARISON OF RAT GINGIVAL FIBROBLAST ATTACHMENT ON COMMERCIAL ACELLULAR DERMAL MATRICES: AN *IN VITRO* STUDY

A Thesis

by

JORDAN CHAY RICHERT

Submitted to the Office of Graduate and Professional Studies of
Texas A&M University
in partial fulfillment of the requirements for the degree of

MASTER OF SCIENCE

Chair of Committee,	Kathy Svoboda
Committee Members,	David Kerns
	Jeffrey Rossmann
Head of Department,	Larry Bellinger

May 2016

Major Subject: Oral Biology

ABSTRACT

Gingival recession is defined as a mucogingival deformity in which the marginal soft tissues are positioned apical to cemento-enamel junction, with concomitant loss of attached gingiva and exposure of root surfaces. Surgical correction to obtain root coverage can be done in several ways including, sliding flaps, free gingival grafts, connective tissue grafts, coronally advanced flaps, or allografts. The purpose of this study was to characterize *in vitro*, fibroblast viability, and morphological appearance, when grown on three commercial acellular dermal matrices used in gingival grafting.

Acellular dermal matrices were tested AlloDerm® RTM (BioHorizons, Birmingham, AL), Puros Dermis (Zimmer Dental, Carlsbad, CA), and PerioDerm™ (Dentsply Implants, Watham, MA). Primary rat gingival fibroblasts were cultured and used between the second and fourth passage for all experiments. All dermal matrices were obtained as packaged for surgical use, cut into 4 mm x 4mm squares, rehydrated in 0.9% sterile saline, and seeded with 3.5×10^5 cells to 4.0×10^5 cells/well. Cells were cultured for 24 hours, 1 week, and 2 weeks in media containing DMEM, 10% fetal bovine serum, and 1% antibiotic/antimycotic. The samples for each dermal matrix per time point (n=3) were either harvested for viability/morphology using confocal, scanning electron, and light microscopy. The samples harvested for viability where stained with live/dead fluorescent dye immediately after culture. The samples harvested for morphology were fixed in 4% paraformaldehyde for 30 minutes, washed and processed for scanning electron microscopy (SEM) or hemotoxylin and eosin (H&E) staining.

All three dermal matrix products appeared to facilitate cell growth. Viability determined via live/dead assay revealed no significant differences between groups. Histologic examination showed fibroblasts throughout various layers of the dermis. SEM data revealed that as time progressed, the matrices exhibited a smoother topography, with dead cells and cellular extensions visualized at higher magnification.

All commercial acellular dermal matrices supported rat gingival fibroblast growth. There were no significant differences in cell viability or cell distribution based on live/dead assay and H&E sections. SEM data supported the theory that fibroblasts consumed and remodeled all acellular dermal matrices.

DEDICATION

I dedicate my thesis to my mother, Janyce, who always supported me throughout my academic career.

ACKNOWLEDGEMENTS

Acknowledgements must truly be given to Dr. Kathy Svoboda, my mentor; this project could not have been accomplished without her guidance and dedication. Thanks to all my additional committee members for their role in guiding my project.

NOMENCLATURE

ADM	AlloDerm® Regnerative Tissue Matrix
CEJ	Cemento-enamel junction
CTG	Connective tissue graft
FGG	Free gingival graft
GTR	Guided tissue regeneration
MGJ	Mucogingival junction
PDM	Puros Dermis
PEM	PerioDerm™

TABLE OF CONTENTS

LIST OF FIGURES

LIST OF TABLES

CHAPTER I

INTRODUCTION AND LITERATURE REVIEW

Gingival Anatomy

The gingiva is part of the oral mucosa that covers the alveolar process of the jaws and the necks/cervical areas of the teeth.[1] In adults, the gingiva normally covers the roots up to the cemento-enamel junction (CEJ), the area of union between the dentin and cementum.[1, 2] Gingiva can be further subdivided into marginal, attached, or interdental areas.[1]

The marginal gingiva, or unattached gingiva, is at the terminal border and surrounds the teeth in a collar-like fashion. The crevice between the marginal gingival and enamel is call the gingival sulcus. Continuous with the marginal gingiva is the attached gingiva, which is firm, resilient, and attached to the periosteum of the underlying bone. The attached gingiva extends to the mucogingingival junction on the facial aspect of the maxilla, as well as on the facial and lingual aspect of the mandible; the palatal surface of the attached gingival blends seamlessly into the palatal mucosa. The interdental gingiva occupies the gingival embrasure, which is the interproximal space between the contact area between teeth. The interdental tissue is pyramidal in shape with the apex located below the contact, continuous from the facial to lingual/palatal aspect. Directly beneath the contact is a saucer-like depression called the col.

Histologically, the outer portions, or oral aspect, of the marginal gingiva, attached gingiva, and interdental areas, are lined with a keratinized stratified squamous epithelium. In contrast, the sulcular epithelium gingival cols are lined with non-keratinized stratified squamous epithelium. At the apical termination of the sulcus lies the junction epithelium. The junctional epithelium is also composed of non-keratinized stratified squamous epithelium, consisting of up to 30 cells thick at the coronal aspect near the sulcus, with as few as one cell at the apex. The junctional epithelium has two basal laminas; an internal basal lamina which faces the tooth, and an external basal lamina that faces the connective tissue.

Gingival Recession

Gingival recession is defined as a mucogingival deformity in which the marginal soft tissues are positioned apical to cemento-enamel junction, with concomitant loss of attached gingiva and exposure of root surfaces.[2, 3] Recession measurements combined with probing depth values are used to calculate clinical attachment levels around teeth, ultimately determining the severity of periodontal disease.[4] Etiologic factors leading to recession can be divided into four main categories: 1) periodontal disease, 2) mechanical forces, 3) iatrogenic factors, and 4) anatomic factors.[5]

Periodontal disease results from a multi-factorial interaction between specific bacterial species and the host immune response.[6, 7] Unresolved periodontal lesions can progress through various stages of inflammation and tissue destruction, eventually resulting in loss of bone, connective tissue, and periodontal ligament attachment. [6]

Clinically this change is evident by formation of periodontal pockets, recession, tissue erythema and edema, and subsequent bleeding upon probing. [6, 8] While gingival recession is normally preceded by a lack of alveolar bone at the site, it is also theorized that the localized inflammation induces sulcular epithelial proliferation into lamina propria of the connective tissue, decreasing the zone of connective tissue between the oral and sulcular epithelium, subsequently leading to recession.[8, 9]

Mechanical forces related to recession are predominately attributed to aggressive oral hygiene practices coupled with faulty tooth brushing technique.[10-12] While the marginal tissues are free of inflammation, the apical displacement of the marginal gingiva denudes the root surfaces. Mechanical irritation due to smokeless tobacco use is also associated with an increased prevalence of recession.[13, 14] Although rare, recession due to factitial injury, particularly fingernail picking, is also reported in the literature.[15, 16] Animal studies indicate that occlusal traumatism is a risk factor for recession and other mucogingival issues.[17, 18] However, some human studies failed to show such an association between occlusal discrepancies and recession.[19, 20]

Iatrogenic factors affecting recession can be subdivided into orthodontic movement and restorative dentistry. Orthodontic movement of teeth out of the alveolar housing can result in bony dehiscences and loss of the alveolar plate, followed by recession.[21, 22] Subgingival placement of crown margins, or packing of impression cord too apically, can result in localized recession.[23] In addition, poorly designed partial denture frameworks coupled with over-extended acrylic can also create localized recession defects around abutment teeth.[24]

Anatomic factors related to recession can include both hard and soft tissue varieties. Most commonly associated with recession is a narrow band of keratinized tissue. [25] Recession defects in areas with inadequate widths of keratinized tissue can be stable and not recede further, when proper periodontal maintenance schedules are followed.[26, 27] However, in patients who discontinue or sporadically attend maintenance appointments, inflammation ensues and recession progresses, in the absence of good plaque control.[28] In a case series report, Stoner and Mazdyasna suggested that high frenum pull was strongly associated with recession, particularly in the mandibular anterior region.[29] Hard tissue factors such as alveolar bone dehiscences can develop due to tooth eruption in the facial or lingual direction, thus predisposing to recession.[9, 12, 25]

Recession defects are classified by defect morphology, extent of the soft tissue and bone loss, and tooth position. Sullivan and Atkins classified recession defects into four categories based primary on defect morphology: 1) deep (more than 3mm) and wide (larger than 3mm); 2) shallow and wide; 3) deep and narrow; and 4) shallow and narrow. [30, 31] Miller later classified recession defects based on extent of soft tissue and bone loss, and tooth position. [32] Class I defects involve marginal tissue recession that does not extend beyond the mucogingival junction, with no loss of interdental bone or soft tissue. Following grafting of class I defects, 100% root coverage is possible. Class II defects involve marginal tissue recession extending beyond the mucogingival junction, with no loss of interdental bone or soft tissue. Following grafting of class II defects, 100% root coverage is possible. Class III defects involve marginal soft tissue recession extending to or beyond the mucogingival junction, with interdental bone and soft tissue loss or with

malpositioned teeth. Following grafting of class III defects, only partial root coverage is usually expected. Class IV defects involve marginal soft tissue recession extending to or beyond the mucogingival junction, with severe interdental bone and soft tissue loss or with malpositioned teeth. Following grafting of class IV defects, no root coverage can be expected.

Epidemiologic studies show recession in populations with both high and low oral hygiene levels.[12, 33, 34] Estimates based on the third National Health and Nutrition Survey (NHANES III) found that approximately 22% percent of the United States' (U.S.) population exhibits one or more tooth surfaces with ≥3 mm of recession.[35] Comparison by gender and ethnicity revealed that recession was significantly greater in men, as well as greater in blacks, when compared to whites and Mexican Americans. Recession was most commonly observed for maxillary first molars and mandibular incisors, with the highest prevalence noted on the buccal/facial aspect of sites. General trends point toward an increase in prevalence, extent, and severity with age. Similar relationships were noted in Swedish cohorts followed for a period of 12 years, with maxillary and mandibular molars and premolars most commonly affected. [34] In addition, 87% of sites that exhibited recession at baseline developed further recession at follow-up, compared to the 33% of unaffected sites that developed recession, indicating that untreated recession is susceptible to further breakdown. Other studies found that, depending on age, the prevalence of recession ranged from 60% to 90% in Norwegians, compared with 30% to 100% in parallel cohorts of Sri Lankans.[33]

Surgical treatment for gingival recession should be considered when the patient is experiencing root sensitivity, is prone to root caries, or is progressively receeding.[35-37] Treatment should also be rendered where there is a lack of keratinized attached tissue, or when driven by the esthetic demands of the patient. Surgical correction of recession defects by gingival grafting is primarily aimed at obtaining root coverage, and includes free sliding flaps[38, 39], double papilla grafts[40], free gingival grafts (FGG)[41, 42], coronally positioned flaps[43, 44], coronal repositioning of a previously placed FGG[45, 46], connective tissue grafts (CTG)[47], guided tissue regeneration[48-50], and allografts. [51]

Gingival Grafting

Grupe and Warren published their sliding flap technique, also known as the lateral positioned pedicle, in 1956, as a treatment for isolated gingival defects. The technique involves vertical incisions created on each side of the defect, connected by a horizontal incision at the base, with the inflamed unattached tissue removed. Full thickness dissection is utilized throughout the attached tissue, followed by split thickness dissection past the mucogingival junction (MGJ). The free flap is then moved laterally to cover the adjacent defect, leaving exposed bone at the donor site to granulate in. The percent of root coverage ranges from 69% to 72%. [5, 52] The advantages of this technique are that it is relatively quick, produces outstanding esthetic results, and does not require a second surgical site.[5] However, this technique is only adequate for single-site defects, can cause recession at the donor site, and requires adequate keratinized tissue and vestibular depth at the neighboring site.

Histologically, the full thickness pedicle heals with a connective tissue attachment in the apical half of the defect, combined with long junctional epithelium in the coronal half. [38] Later modifications of this technique incorporated a partial thickness pedicle, thus leaving a layer of periosteum over the donor site. However, histologically, only a long junctional epithelium was established, with no connective tissue attachment observed.

Cohen and Ross developed the double papilla repositioned graft in 1968 an alternative to the laterally positioned pedicle flap.[40] The technique involves removal of a "V" shaped wedged of tissue at the gingival margin of the defect, followed by vertical incisions at the line angles, turning obliquely down to the mucosa. The oblique incisions are connected by inserting a blade into the underlying submucosa in a horizontal fashion. The two papillae are then dissected from the periosteum in split thickness approach, rotated over the recipient site, and sutured together. The advantages of this technique is that it includes minimal exposure of underlying tissue following donor harvest, reduction in tension and pull of the flap, additional blood supply to the flap, and greater quantity of the gingiva displaced from the interdental surfaces over the recipient site. Nonetheless, this procedure is very technique sensitive, and presents with poor predictability for root coverage.[5]

Björn first published on the free gingival graft (FGG) in Sweden in 1963, but Pennel and King were the first to present the technique in the United States in 1964.[53-55] Free gingival grafts were initially used in periodontal therapy to increase the zone of keratinized tissue around teeth, as well as to extend the depth of the vestibule.

Eventually, FGGs became more widely used for root coverage following the publication of Miller's classification system.[32]

In 1968, Sullivan and Atkins outlined the successful principles for free autogenous gingival grafting.[30, 31] Briefly, the recipient sites' epithelium, connective tissue, and muscle fibers are removed down to the periosteum, thus creating a bleeding bed for the graft. Donor tissue is most commonly taken from the palate. Every FGG harvested from the palate includes the epithelium, as well as varying portions of the lamina propria. Full-thickness grafts include the entire lamina propria, while split-thickness grafts include only part of it. Split thickness grafts are categorized as intermediate or thick, and range in thickness from 0.5 mm to 0.75 mm, and 0.75mm to 1.25mm, respectively. Full-thickness grafts range in thickness from 1.25 mm to 1.75 mm. The thicker the graft, the greater the degree of primary graft contraction, while the thinner the graft, the greater the degree of secondary contraction. The graft dimensions should be calculated based on the dimensional requirements of the recipient site, and extended slightly to account for graft shrinkage immediately after separation from the palate. The donor site can then be covered with a vacuform surgical stent to aid in clot formation and hemostasis. The graft is then quickly transferred to the recipient site, and sutured into place at the periphery. Compression sutures may also be placed over the site to facilitate intimate contact between the graft and the recipient bed. Surgical dressing may be placed over the site but is optional. Mean root coverage in a FGG is 88%, with total root coverage ranging from 70-90%. [32, 41, 56] The advantages of this technique is that it is relatively quick, can be used for multiple recession defects, is not dependent on

adjacent donor tissue, and is not dependent on vestibular depth. [5] The disadvantages include pain and bleeding at the donor site as well as esthetic discrepancies related to the lightness of the graft following complete healing.

Another important hallmark of the Sullivan and Atkins series was the description of the stages of graft "take" or incorporation.[30, 31] The first stage of graft incorporation is plasmatic circulation, which occurs within the first two days, during which the graft is solely dependent upon diffusion from the host bed through the fibrin clot. The stage of revascularization takes place between the second and eighth day, and is characterized by capillary extension into the graft. While capillary proliferation begins after the first day, adequate circulation does not occur until the eighth day. Concomitant with vascularization, the stage of organic union occurs between the fourth and tenth day, and is defined by the connective tissue union between the graft and recipient bed.

Pasquinelli described the histology of the new attachment formed 10.5 months after the treatment of a deep recession defect with an FGG. [57] He showed varying zones of new bone formation with mature osteocyte lacunae parallel to the tooth at the base, contrasting with large irregular lacunae at the coronal aspect. In addition, the bone in the coronal aspect appeared to have a collagenous pattern, with a surrounding hypercellular osteoid matrix filled with large, pale, dentritic appearing osteoblasts. Cementoid tissue appeared to be deposited on old cementum in the most coronal aspect, with new mature cementum with perpendicular inserting connective tissue fibers just below. New cementum did not appear to be deposited directly on dentin. New connective tissue attachment extended apically from the long junctional epithelium down to the osseous

crest; however due to artifactual separation of the specimen, portions of the attachment could not be described. Overall the histologic evidence showed that treatment of a gingival recession defect with a FGG could result in some regeneration of bone, cementum, and connective tissue.

For single teeth exhibiting shallow recession, coronally advanced or repositioned flaps are indicated.[5] Potential sites must not exhibit bone loss, and present with adequate keratinized tissue width and thickness.[43] Various techniques exist in which to accomplish advancement. Traditionally, vertical incisions are made at the line angles of the defects with full-thickness flap reflection, and advancement with a partial-thickness periosteal release. The flap is then sutured at the CEJ. One study reports mean root coverage of 97.8% at six months.[43] Alternatively, a semilunar coronally repositioned flap may be used.[44] The same requirements of coronally advanced flap are applicable with this technique as well. Essentially, a submarginal semilunar incision is placed on bone, following the curvature of the free gingival margin. A second sulcular incision is made, connecting with the base of the flap in a split-thickness fashion. The flap is advanced, leaving periosteum exposed. Pressure at the site stabilizes the blot clot, thus sutures are not required. In the event that adequate keratinized tissue is not present, a FGG will need to be placed first, and allowed to heal for at least two months, before coronal advancement.[45, 46]

While each procedure has its indication as it relates to soft tissue augmentation, the subepithelial connective tissue graft (CTG) is considered to be the gold standard in attaining root coverage.[58] Langer and Langer described the surgical technique in detail

for successful connective tissue grafting for root coverage.[47] Essentially, the recipient bed is prepared by placing two vertical incisions one tooth mesial and distal to the defect with horizontal sulcular incisions at the crest. The base of the flap is released by split thickness dissection to allow for coronal advancement. The donor site is accessed by placing a horizontal incision in the palate, five to six millimeters from the gingival margin toward the alveolar bone. The length of the incisions is dependent on the combined widths of the recession defects. A second incision is made two millimeters coronal to the first, connecting on the alveolar bone, and scoring the periosteum. If required, vertical incisions can be made on the mesial and distal aspects to help facilitate removal of the connective tissue wedge. The palate is sutured immediately. Collagen can be placed in the soft tissue void between the first two horizontal incisions, and periodontal dressing can be applied. The epithelial collar can be excised prior to graft placement or can be left attached and exposed after suturing, to allow for additional keratinized epithelium. The connective tissue is sutured over the denuded roots, and the flap is advanced as much as possible over the graft. Bruno later developed the single incision palatal harvest, while Zucchelli pioneered an envelope flap technique that did not require vertical incisions.[59, 60] Complete root coverage ranges from 8.6% to 96.1% while mean root coverage ranges from 65.4% to 97.3%.[58]

Guiha studied the healing and revascularization of subepithelial connective tissue grafts in beagle dogs. [61] At 7 days post-surgery, a blood clot was present between the graft and the periosteum, and between the graft and the flap, trapping red blood cells and inflammatory infiltrate within the immature fibers. The orientation of these immature

fibers was similar to that of the flap, but in a different direction compared to that of the graft. During this time period, blood vessels from the periosteum began to invade the graft, and capillaries within the periodontal ligament appeared engorged. By the end of 14 days, the oral epithelium had not yet formed, but granulation tissue was noted between the flap and the graft. Also at this time, the graft was completely vascularized; with decreased vascular engorgement in the periodontal ligament and bone. By 28 days, the junctional epithelium had already been established, and there was an increase in the thickness of the sulcular epithelium. The demarcation between the flap and the graft, and the graft and the periosteum, could no longer be visualized. Flap microvasculature appeared almost normal, with full restoration of the subepithelial, crevicular, periodontal, and supraperiosteal plexi. By 60 days, the epithelium had regained its normal shape, thickness, and appearance, with dense connective tissue fibers noted throughout. Full vascular maturation was also complete at this point in time.

Bruno described the histology of the new attachment formed 12 months after the treatment of a recession defects with a CTG.[62] He noted that exposed root surfaces were predominantly covered with connective tissue, in intimate contact with the dentinal tubules. The nature of this attachment is suggested to be a connective tissue adhesion. Harris, however, observed connective tissue fibers inserting directly into the cementum, dentin, and bone.[63] Both authors noted that at the base of the recession defect, attachment occurred via periodontal regeneration of the cementum, PDL, and bone, with nuclei visualized in the lacunae of the new bone.[62, 63] Goldstein found similar evidence of periodontal regeneration at select portions of the CTG site 14 months post-surgery.[64]

Cummings noted a disorganized connective tissue attachment parallel to the root surface, observing cemental deposition in some specimens, but not complete regeneration.[65] Most CTG's are not uniform, and commonly contain adipose tissue from the submucosal layer of the palate, which can also be incorporated into the grafted site.[65, 66]

Guided tissue regeneration (GTR) describes a class of procedures designed to regenerate lost periodontal structures including bone, cementum, and periodontal ligament, by utilizing barrier techniques to exclude epithelium,.[2] Studies have attempted to regenerate lost periodontal tissue attachment around recession defects using a combination of resorbable and non-resorbable barrier membranes.[48-50] Early studies by Tinti utilized non-resorbable membranes, placing them over the defects, and coronally advancing the flap over the surface. [48] Membranes were removed four weeks later, and at six months post-operatively, significant differences in recession reduction and clinical attachment gain were noted. Pine-Prato incorporated a similar approach using resorbable membranes composed of polygalactic acid and citric acid esters.[49] Again, the membranes were placed over defects with the flap coronally advanced over the top. At six months post-operatively, significant improvements were noted for clinical attachment gain and recession coverage compared to baseline values. Rocuzzo later compared both types of membranes in the treatment of human gingival recession. Significant improvements in clinical attachment gain and probing depth reduction were noted for each group between baseline and 6 months post-operatively. However, mean root coverage was comparable for both groups, with non-resorbable membranes and resorbable membranes achieving 83.2% and 82.4% coverage, respectively.[50] Long-term stability following GTR

procedures can vary greatly. Pine-Prato obtained four year post-operative measurements for cases treated with non-resorbable membranes.[67] Over time, root coverage remained stable, in addition to a significant increase in the amount of keratinized tissue, which developed as the mucogingival junction migrated apically. Conversely, Harris re-examined cases treated with resorbable membranes at 25.3 months post-operatively.[68] He noted a significant reduction in root coverage, from 92.3% coverage at six months, to 58.8% at two years, indicating that GTR may not provide long-term stability.

Cortellini examined block histology following GTR with a non-resorbable barrier membrane.[69] The membrane was left in place for 5 weeks with specimen sectioning completed at 5 months. Histology demonstrated newly formed bone and cementum coronal to the most apical extent of root instrumentation. Connective tissue attached to three-fourths of the newly formed tissue, with junctional epithelium accounting for the most coronal portion of the attachment. The majority of these grafting procedures require a donor site for autogenous tissue, necessitating a second surgical procedure for harvesting. Particularly with the CTG, a second surgical procedure for harvest can prolong chair time, increase tissue morbidity, and increase intra and/or post-operative discomfort.[70] Additionally, the availability of autogenous tissue is limited, restricting the number of recession defects that can be covered in a single surgery. Allograft materials offer an alternative to such a problem.

It is worth noting that many of the studies vary in the way in which they evaluate the post-operative success of surgical techniques and materials. Some studies refer to root coverage, which is the portion of the root covered by tissue post-operatively, while

others refer to defect coverage, the portion of the defect covered after a grafting. For standardization, Greenwell suggested that the success of root coverage procedures should be based on a mean root length 13.63 mm, which would allow for simultaneous evaluation of both defect coverage and defect elimination of a surgical technique[71] Thus, a residual 1 mm recession defect would always result in 93% root coverage, and a 6 mm residual defect would always be result 56% root coverage.[71]

Allografts

Allograft substitutes used for root coverage procedures are harvested from cadavers and processed to remove all cellular components. Of the current products on the market, AlloDerm® Regenerative Tissue Matrix (ADM) (BioHorizons, Birmingham, AL) is the longest used and most studied.[72] The ADM tissues are obtained from independent third-party American Association of Tissue Banks (AATB) guideline-compliant facilities. Tissues are transported in culture media containing various concentrations of gentamicin, cefoxitin, lincomycin, polymyxin B, and vancomycin.[73] Donor blood is tested for HIV and hepatitis B and C, and tissue samples are screened for microbial contaminants; tissues must be free of pathogenic bacteria prior to acceptance.[72] The ADM allograft undergoes a 3-step proprietary process to prepare the tissue for transplantation. First, a high-ionic strength solution is used to uncouple the intercellular bonds between layers, separating the dermis from the epidermis, leaving the basement membrane intact. [73-75] Secondary washing with sodium deoxycholate then de-cellularizes the dermis, removing donor major histocompatibility class I and II antigens.

[73, 75, 76] The final step involves a unique freeze-drying process that creates an amorphous ice that retains the structural integrity of the complex microarchitecture of the dermis. [75] The remaining dermal matrix contains glycosaminoglycans along with undamaged fibers and bundles of type I, III, IV and VII collagen, laminin, and elastin.[73-75, 77] The matrix acts as a scaffold, promoting epithelial migration along the basal lamina, with in-growth of fibroblasts and endothelial cells along the porous dermal aspect.[73, 78] The ADM allograft arrives sealed within two 2 Tyvek backs, containing trace amounts of antibiotics.[79] The tissue must be rehydrated in two saline baths, for a total rehydration time of 10 to 40 minutes. The final thickness ranges from 0.9mm to 1.6mm.[80]

Clinically, ADM heals similarly to a CTG, with no significant differences noted in regards to recession coverage, keratinized tissue, probing depth, and clinical attachment levels.[81] Histologically, the gingival attachment is similar, with both grafts exhibiting a long junctional epithelium and connective tissue adhesion.[65] Both grafts incorporate well within recipient tissues, with new fibroblasts, endothelial cells, and collagen dispersed throughout. ADM, however, contains more elastin than a CTG, which is only evident histologically.[65, 82]

Another acellular dermal allograft material, Puros Dermis (PDM) (Zimmer Dental, Carlsbad, CA), has been marketed as an alternative to autogenous soft tissue grafting, both for root coverage, and for horizontal/vertical soft tissue augmentation.[83] This allograft retains its natural collagen matrix along with the mechanical properties of native dermis. The tissue is processed via a proprietary Tutoplast process. The Tutoplast process is a multi-stage method that utilizes solvent-dehydration in conjunction with

gamma irradiation in lieu of freeze-drying.[84] The initial phase incorporates an osmotic treatment to kill bacteria and reduce viral load.[83] This is followed by an oxidative treatment to destroy remaining proteins and minimize graft rejection. A solvent-dehydration step then removes water and further disinfects the matrix and reduces prions. The final step incorporates limited-dose gamma irradiation to provide a level of sterility of 10^{-6}. The tissue is delivered in a doubly sealed package, and is reported to rehydrate in 30 seconds but can be rehydrated for up to 30 minutes to improve handling properties.[85, 86] The final tissue thickness ranges from 0.8mm to 1.8mm.[83]

A review of the literature revealed two studies that evaluated PDM in the clinical healing of root coverage. The first split-mouth clinical study compared PDM with ADM in Miller Class I and III recession defects.[86] The percentage of root coverage was 81.4% for PDM, and 83.4% for ADM, a difference which was not significant. A second multicenter study compared PDM with ADM in Miller Class I and II recession defects.[87] The percentage of root coverage for the PDM and ADM were 77.2% and 71.01% respectively. Again, these differences were not significant. Histologic evaluation was not performed in either publication and no histologic studies were found within the body of literature.

The most recently launched acellular dermal allograft is PerioDerm™ (PEM) (Dentsply Implants, Watham, MA). Like its predecessors, it has been recommended for root coverage and supplemental support for soft tissue defects. [88] Tissue procurement is done through the Musculoskeletal Transplant Foundation (MTF), which exceeds the standards of AATB. Aside from screening donors for cancer and illegal drug use, the

donor's blood is also tested for hepatitis B and C, HIV, and syphilis. The tissue is minimally processed to remove epidermal and dermal cells while maintaining the integrity of the extracellular matrix. The three-phase proprietary processing includes an initial treatment of sodium chloride, which separates the dermis from the epidermis. The dermis is then washed with Triton, a detergent that removes any remaining cellular debris. The last phase includes propriety disinfection and freeze-drying, reducing bacteria and fungi to 10^{-6} and viral load from 10^{-4} to 10^{-6}. No sensitizing agents or β-lactam antibiotics are used in the processing.[89] The tissue is doubly packaged in Tyvek bags, and requires only 3 to 5 minutes of rehydration in sterile saline or lactated Ringer's solution. Final tissue thickness ranges from 0.8mm to 1.7mm.

At this time there are no peer-reviewed articles in the literature regarding the clinical application of PEM. In addition, there are no published studies examining the histology of the PDM allograft. However, a non-controlled case study is available through the distributer's website.[88]

Acellular dermal matrices, specifically ADM, have also been used in conjunction with biologics to increase post-treatment success. Shin compared root coverage with ADM with and without enamel matrix derivative.[90] He found that the use of enamel matrix derivative significantly increased keratinized tissue but did not affect probing attachment levels or percentage of root coverage. Carney compared root coverage using ADM with and without the use of human platelet-derived growth factor.[91] He found no statistical differences in keratinized tissue, probing attachment levels, or root coverage.

CHAPTER II

STUDY DESIGN

Background to Issue

Type I collagen is the predominant component of AlloDerm® (ADM), Puros Dermis (PDM), and PerioDerm™ (PEM) allografts tested; its fibrillar structure is essential for fibroblast attachment, proliferation, and differentiation, and.[92] Type I collagen is also the most abundant collagen within the periodontium, accounting for 80% to 85% of the collagen within gingiva[1]. Cell-to-cell interaction and cellular attachment to the extracellular matrix (ECM) are mediated by large heterodimeric membrane glycoproteins known as integrins.[93] Integrins consist of 1α and 1β subunit, with α1β1 and α2β1 representing the major collagen receptors in fibroblasts. Integrins are also associated with intracellular focal adhesion proteins vinculin, talin, and paxillin.[94] Vinculin and talin are linked to the actin cytoskeleton, while paxillin, a signaling/adapter protein, binds to vinculin through a series of kinases.[95] Integrins and adhesion plaques can form classical focal adhesions, which are flat elongated structures along at the periphery of cells.[96, 97] Additional configurations include fibrillar adhesions, which are even more elongated, and focal complexes, which appear as small, dot-like structures.[98-101]

Various methods for examining human gingival fibroblast interactions with collagen matrices/scaffolds have included light microscopy, confocal, and scanning electron microscopy (SEM).[102, 103] While conventional light microscopy and SEM are

suitable methods for examination, they only characterize a single layer or surface of the specimen, and often require sectioning of the specimen to observe multiple levels. Confocal microscopy, on the other hand, utilizes fluorescent labeling and z stack imaging to layer images on top of one another without compromising the integrity of the specimen.[103] Confocal microscopy is often used in conjunction with live/dead assays to test for cellular viability.[104] Live and dead cells will fluoresce at different wavelengths, allowing for easy quantification by measuring fluorescent pixel intensity via imaging software.

Each of the above soft tissue allografts utilize proprietary processing to provide a stable dermal matrix devoid of cellular components. While numerous studies have demonstrated that ADM is comparable to a connective tissue graft (CTG), only two studies have compared PDM to ADM, and no studies have compared either allograft to the PDM allograft. It is unclear how tissue processing affects graft integration, and if these differences affect local host cell infiltration into the matrix. Therefore, the purposes of this study are to investigate, *in vitro*, rat gingival fibroblast 1) viability 2) and morphology when grown on three commercial acellular dermal matrices used for gingival grafting.

Materials and Methods

Primary Cell Culture

Rat gingival fibroblasts (RGFs) were harvested post-mortem from the palates of female Sprague Dawley rats. The explants were dissected into pieces 2-3 mm in

diameter and plated on tissue-culture Petri dishes (Falcon™ BD Biosciences Discovery Labware, Bedford, MA, USA) with high-glucose Dulbecco's modified Eagle's medium (DMEM), 10% fetal bovine serum (FBS), and 1% antimycotic/antibiotic.[105] Incubation at 37ºC in a humidified gas mixture environment (5% CO_2, 95% air), with growth medium changed every 48 hours was done. After 3-4 weeks, the explants were removed and cells attached to the dish were passaged using 2-3ml of 0.25% trypsin-EDTA (Sigma-Aldrich, St. Louis, MO, USA) solution. Once the cells were detached, the trypsin was neutralized by adding an equal amount of fresh media to the dish. The entire volume of the dish was transferred to a centrifuge tube and spun at 1500 rpm for 3 minutes. The supernatant was removed and the pellet re-suspended in fresh growth media, and subsequently transferred to a T25 (25ml) culture flask (Corning, Corning, NY, USA). Additional culture media was added until the bottom of the flask was covered, resulting in a final volume of five to six milliliters. Passages two though five were utilized for experimentation, with cells of the same passage used within each experiment.

Cell Culture on a 2-Dimensional Surface

The RGFs were plated on eight-well LabTek chamber slides (LabTek II Chamber Slide System, Sterile NUNC-VWR, Secaucus, NJ, USA), suspended in 10µl of high-glucose Dulbecco's modified Eagle's medium (DMEM), 10% fetal bovine serum (FBS), and 1% antimycotic/antibiotic[105], at a density of 3.0×10^5 to 4.0×10^5 cells per chamber. An additional 190 µl of growth medium was added to each chamber for a total volume

of 200 µl per chamber. Incubation took place at 37ºC in a humidified gas mixture environment (5% CO_2, 95% air), with growth medium changed every 48 hours. Incubation periods were 24 hours, 7 days, and 14 days.

Cell Culture on a 3-Dimensional Surface (Acellular Dermal Matrix)

Each acellular dermal matrix was rehydrated per manufacturer's instructions in 0.9% normal saline.[79, 85, 89] Matrix specimens, 4mm x 4mm in dimension, were placed at the bottom of a 96 well culture plate (Corning, Corning, NY, USA), with the dermal aspect up, and pre-incubated in 60 µl of culture medium for 30 minutes prior to seeding. The media was aspirated and RGFs were suspended in 10µl of high-glucose Dulbecco's modified Eagle's medium (DMEM), 10% fetal bovine serum (FBS), and 1% antimycotic/antibiotic[105], at a density of 3.0×10^5 to 4.0×10^5 cells per well. An additional 110 µl of growth medium was added to each chamber for a total volume of 120 µl per well. Incubation took place at 37ºC in a humidified gas mixture environment (5% CO_2, 95% air), with the growth medium changed every 48 hours. Incubation periods were 24 hours, 7 days, and 14 days.

Live/Dead (Viability)

After each specified incubation period, Live/Dead fluorescent dye (Abcam, Cambridge, MA, USA) was diluted with 1X PBS at a final concentration of 5x. A volume of 100 µl was added to each well and incubated for ten minutes. Leica SP5 confocal microscope was used to excite the samples between 480 and 630 nm, and read

using the FITC/TRITC settings in the confocal software. The entire sample was mounted on the slide, but scanning was limited to the areas were cells were present, which on average penetrated 100 μm into the specimen. Live cell dye, calcein AM, labels intact viable cells fluorescent green.[106] It is membrane permeant, passing through intact plasma membranes. The cell remains non-florescent until the intracellular esterases remove ester groups, rendering the area fluorescent green. The dye excites at a maximum wavelength of 494 nm, and emits at 515 nm, respectively. The dead cell dye, propidium iodide, labels cells with compromised plasma membranes. It is membrane impermeant and binds directly to DNA with high affinity. The fluorescence increases 30x when bound to DNA, fluorescing red. The dye excites at a maximum wavelength of 528 nm and emits at 617nm, respectively.

Z stacks were maximally projected into 2D images, and the entire frame was selected as a region of interest (ROI). Data from these images were quantified using the Leica Application Suite, Advanced Fluorescence (LAS-AF) quantifying software by comparing the number/intensity of pixels highlighted in the frame in the desired wavelength channels. Thus, the intensity of the green pixels (live) were compared the intensity of the red pixels (dead). The pixel intensity was converted gray scale values, providing a numerical output. The ratio of green to red (G/R) pixels were calculated for each membrane and compared between and within groups. Three samples, per membrane, per time point, were analyzed, for a total of 27 samples.

Cell Morphology

In order to determine conformation changes in cell morphology for fibroblasts grown on 2-dimensional (2-D) vs. 3-dimensional (3D) surfaces, actin and nuclear staining was performed. After fixation, the cells were washed with 1x PBS for 10 min, after which filamentous actin was be labeled using AlexaFluor phalloidin 488 (green) fluorescent stain (Cell Signaling Technologies, Danvers, MA, USA) at a 1:20 dilution for 15 min for 2-D surfaces, and 30 minutes for 3-D surfaces. A volume of 100 µl was added to each well. The samples were washed with 1X PBS three times over a 15 minute period. The nuclei were then stained with TO-PRO-3 iodide 642 (red) fluorescent stain (Life Technologies, Eugene, OR) at a 1:1000 dilution for 5 minutes. A volume of 100 µl was added to each well. The samples were then again washed with 1X PBS three times over a 15 minute period. Stained samples were mounted in Slowfade Gold anti-fade reagent (Invitrogen). Leica SP5 confocal microscope was used to excite the samples at various wavelengths, using the FITC/TRITC confocal settings to visualize structures. Only samples cultured for two weeks were examined, one chamber was slide compared to each of the three membrane groups.

Scanning Electron Microscopy

Membrane samples were be fixed for 30 minutes with 2% formalin and lightly washed with 1x PBS to ensure complete removal of salts and unattached cells. Sample dehydration was accomplished through a series of ethanol washes for 2 minutes each with increasing concentrations (25%, 50%, 75% and 100%) and desiccated overnight

under vacuum. The samples were sputter-coated with gold (80s, 20 mA) for analysis by scanning electron microscopy (SEM) at an accelerating voltage of 5kv. One to three images per membrane, per time point, was scanned. A hydrated control and an un-hydrated control were also scanned for each of the three matrices. A total of 15 specimens were examined.

Histology

After each specified incubation period, the unattached RGFs were washed off of the membranes using 1X phosphobuffered saline (PBS). Membranes were fixed in 4% paraformaldehyde at 4^{o}C. After dehydration, specimens were immersed in paraffin and processed for sectioning. Paraffin embedded specimens were sectioned at 10 to 15 microns in thickness. Slides were stained with hematoxylin and eosin (H&E) and examined with a wide field light microscope. Three sections per membrane, per time point were stained for a total of nine specimens. The best section for each membrane was photographed using a Zeiss Axioplan microscope with a color digital spot camera, and individually examined for cellular dispersion throughout the matrix.

Statistical Analysis

To analyze the presence of significant differences for G/R ratios at each point of time between each membrane group and within each membrane group, a Kruskal-Wallis Rank Sum Test for Two-Sided One-Way ANOVA was performed. The level of significance was adjusted with Bonferroni corrections to an $\alpha < 0.0056$ (9 groups

compared therefore 0.05/9). Post hoc testing was performed using the Mann-Whitney U two sample comparison to determine inter-group and intra-group differences.

CHAPTER III

RESULTS

Gingival Fibroblast Morphology Was Flat on 2-D Surfaces but Spindle Shaped on 3-D Matrices

Fibroblast growth on the 2-D chamber slide appeared confluent at the 2 week time point (Figure 3-1 A). The cells were flattened morphologically with little overlap, displaying distinct actin and nuclear staining. In contrast, fibroblasts appeared sporadic on the 3-D PDM allograft (Figure 3-1 B). The cells displayed a bipolar stellate morphology, with distinct actin staining, with less obvious nuclear visualization. Overall fibroblast orientation and morphology differed between 2-D and. 3-D culture surfaces.

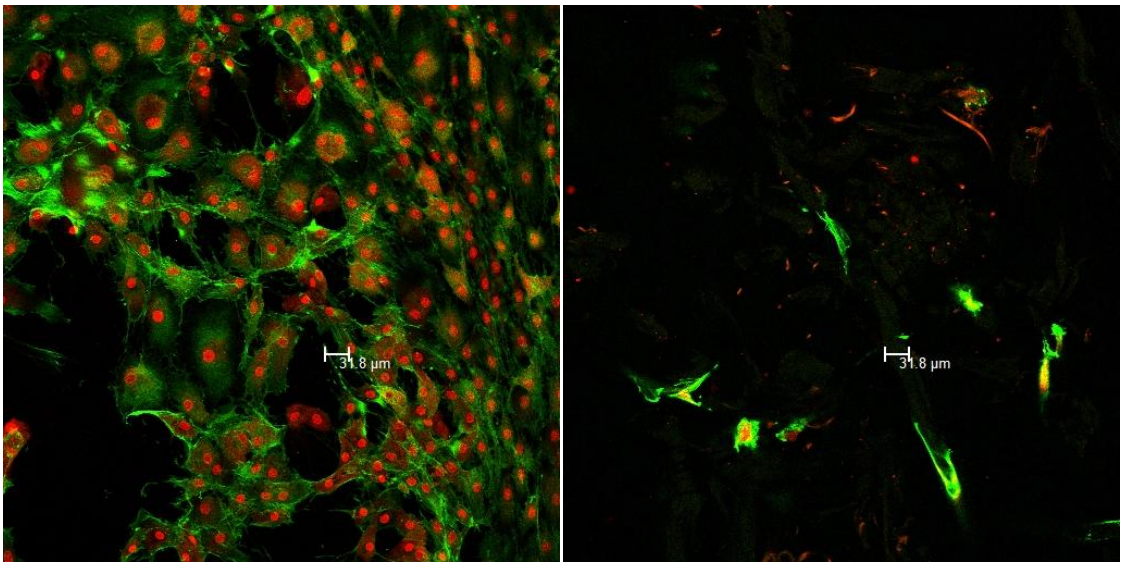

Figure 3-1. Single Z-stack comparison of cell morphology with actin (phalloidin-green) and nuclear staining (To Pro-red). A) 2-D chamber slide, B) 3-D matrix at 2 weeks on the PDM allograft.

All Dermal Matrices Supported Gingival Fibroblasts Viability

The live/dead assay aids in identifying viable cells at the time the specimens are removed from culture. The green dye, calcein AM, permeates through the cell membrane, fluorescing green after intracellular esterases process it. The red dye, propidium iodide, cannot permeate the plasma membrane, and as such will only stain dead cells with compromised membranes, binding to DNA and fluorescing red.

Representative images for the live/dead assay for each membrane at each time point are presented below: 24 hour (Figure 3-2), 1 week (Figure 3-3), and 2 week (Figure 3-4). Visually, both live and dead fibroblasts appeared at multiple levels within each matrix. The PEM group had the highest mean G/R values among the 24 hour and 2 week time points, as well as the highest mean G/R value for the combined time points (Figures 3-2 D, 3-4 D, 3-5 D). However, the ADM group had the highest mean G/R value for the 1 week time point (Figure 3-3 D). Negative trends were noted in the ADM and PDM groups, with the 24 hour time points displaying the highest mean G/R values, with the 2 week time points exhibiting the lowest (Figures 3-2 D, 3-4 D). The PEM group displayed the highest mean G/R values at the 24 hour time point, with the lowest of value observed for the 1 week time point (Figures 3-2 D, 3-3 D, 3-4 D). Box plots demonstrating the range of G/R values were variable for each membrane at each time point, but more evenly distributed when all time points were combined (Figures 3-2 E, 3-3 E, 3-4 E, 3-5 B). Several outliers were noted in the PDM group for the combined time point box plot (Figure 3-6B).

In regards to intra-group comparisons, trends noted in mean G/R values and G/R data distribution were similar to those seen in the intergroup comparisons (Figures 3-6 A, B, 3-7A, B, 3-8 A, B). Negative trends were noted for mean G/R values for the both the ADM and PDM groups, while a bimodal pattern was seen for the PDM group, denoted by the decreasing G/R value at 1 week.

In regards to mean G/R differences between membrane groups for the 24 hour, 1 week, and 2 week time points, no significant differences were noted (Table 3-1). No significant differences were noted between groups when all three time points were combined for each membrane (Table 3-2). Within each membrane group, no significant differences were noted between the 24 hour, 1 week, and 2 week time points (Table 3-1).

Overall, while varying mean G/R values were noted for all membrane groups at all time points, these differences were not significant, indicating that the proportion of live fibroblasts to dead fibroblasts were similar, regardless of the membrane group or time period.

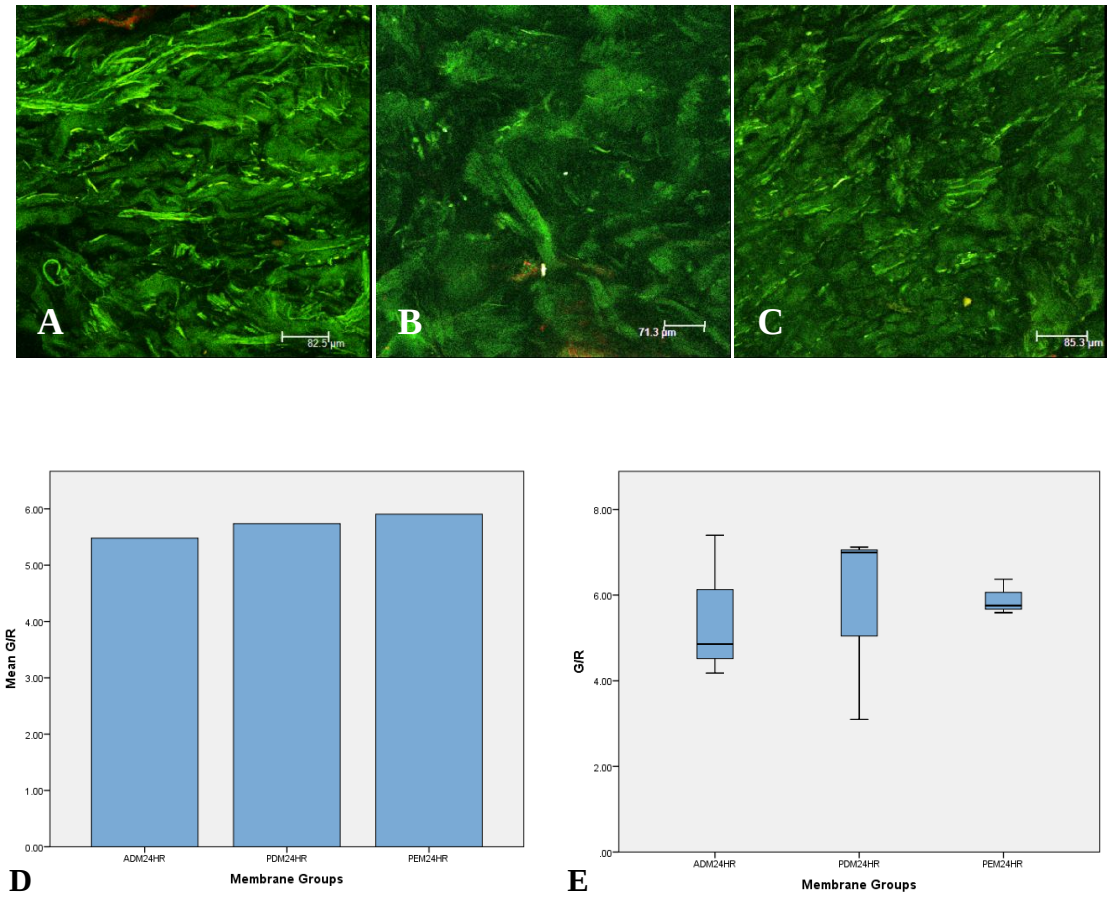

Figure 3-2. Live/dead data for 24 hour time points. A) Max projection ADM, B) Max projection PDM, C) Max projection PEM, D) Bar graph for mean G/R for live/dead assay for 24 hour time points for each membrane group, E) Box plot for G/R values for live/dead assay for 24 hour time points for each membrane group.

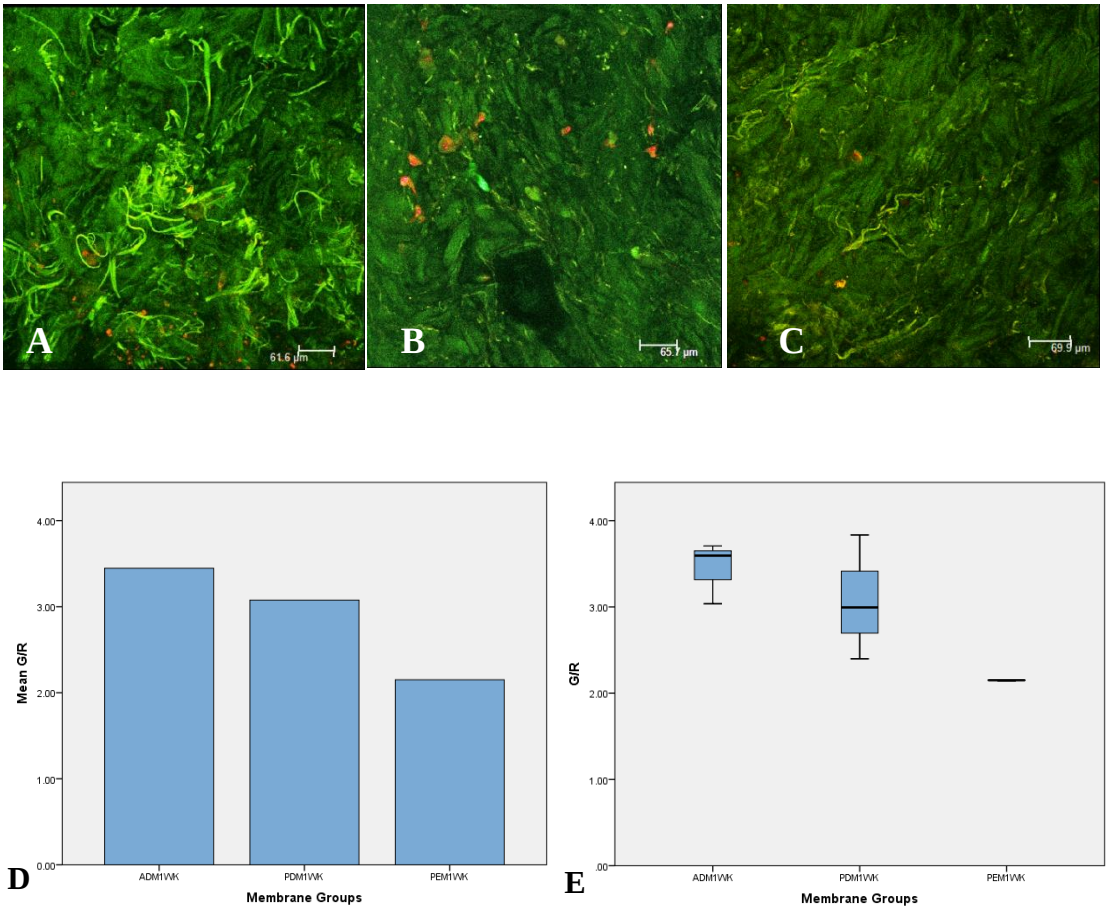

Figure 3-3. Live/dead data for 1 week time points. A) Max projection ADM, B) Max projection PDM, C) Max projection PEM, D) Bar graph for mean G/R for live/dead assay for 1 week time points for each membrane group, E) Box plot for G/R values for live/dead assay for 1 week time points for each membrane group.

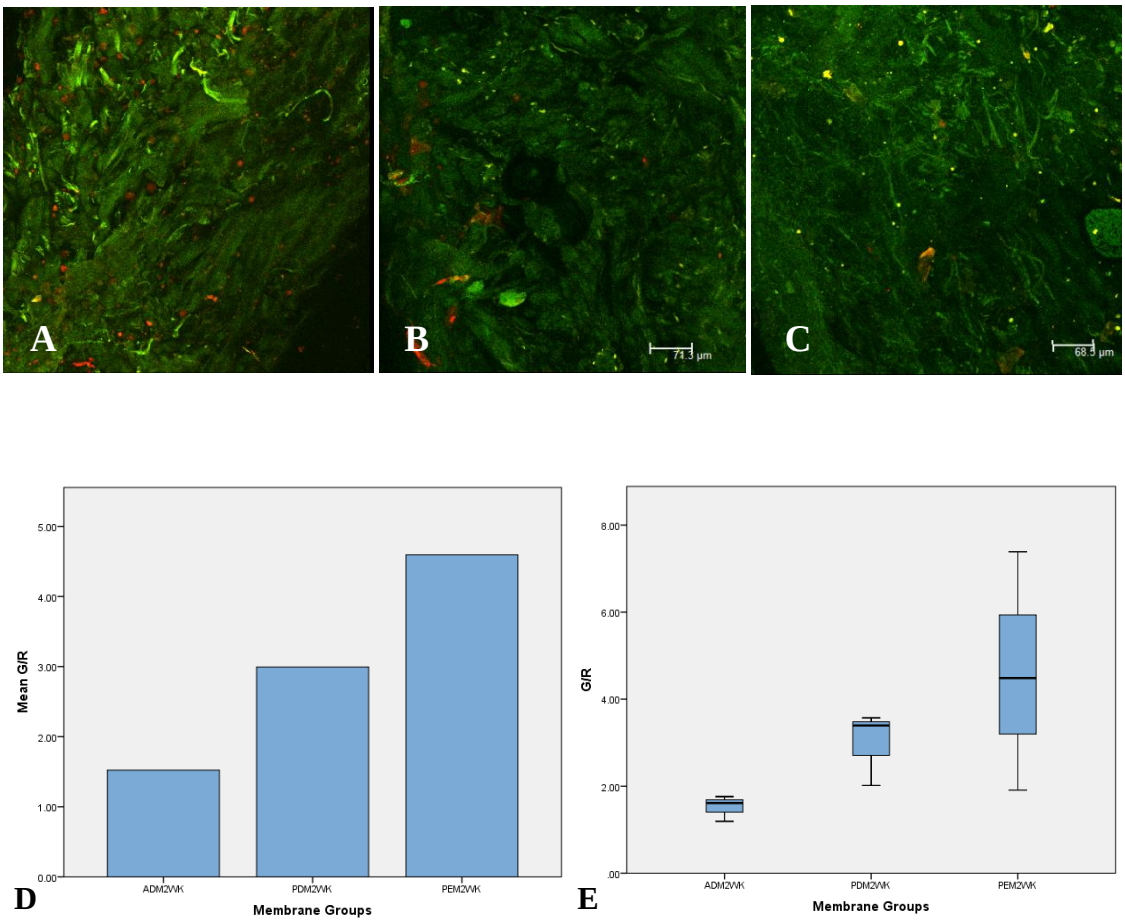

Figure 3-4. Live/dead data for 2 week time points. A) Max projection ADM, B) Max projection PDM, C) Max projection PEM, D) Bar graph for mean G/R for live/dead assay for 2 week time points for each membrane group, E) Box plot for G/R values for live/dead assay for 2 week time points for each membrane group.

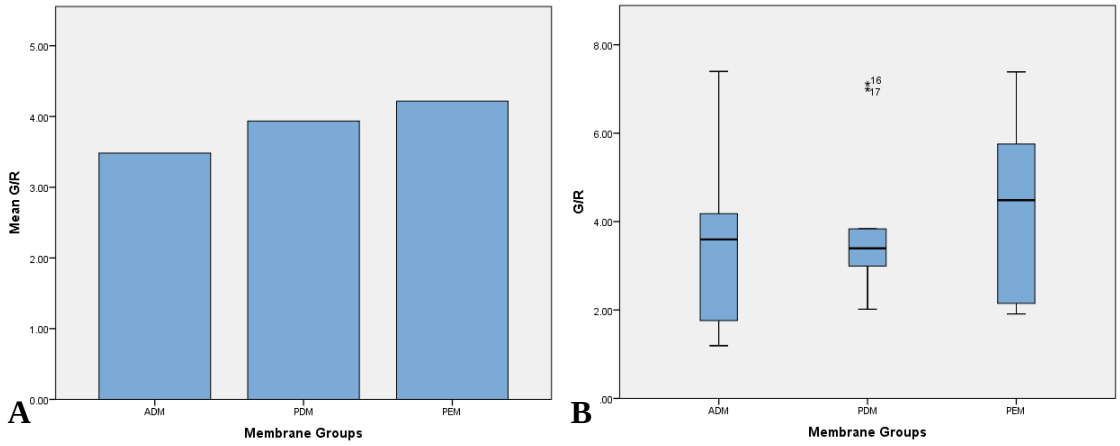

Figure 3-5. Live/dead data for combined time points. A) Bar graph for mean G/R for live/dead assay for combined time points for each membrane group, B) Box plot for G/R values for live/dead assay for combined time points for each membrane group

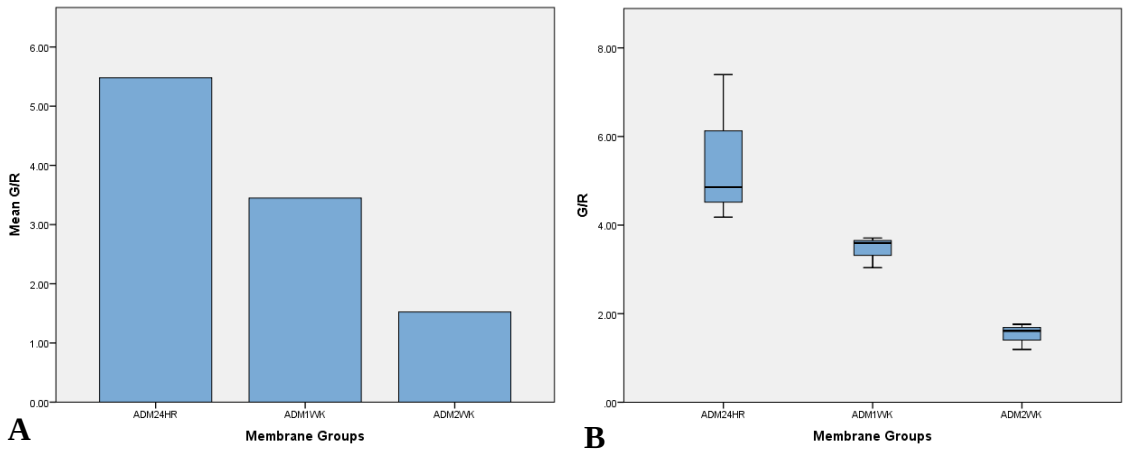

Figure 3-6. Live/dead data for ADM group at each time point. A) Bar graph for mean G/R for live/dead assay for each time point for ADM group, B) Box plot for G/R values for live/dead assay for each time point for ADM group.

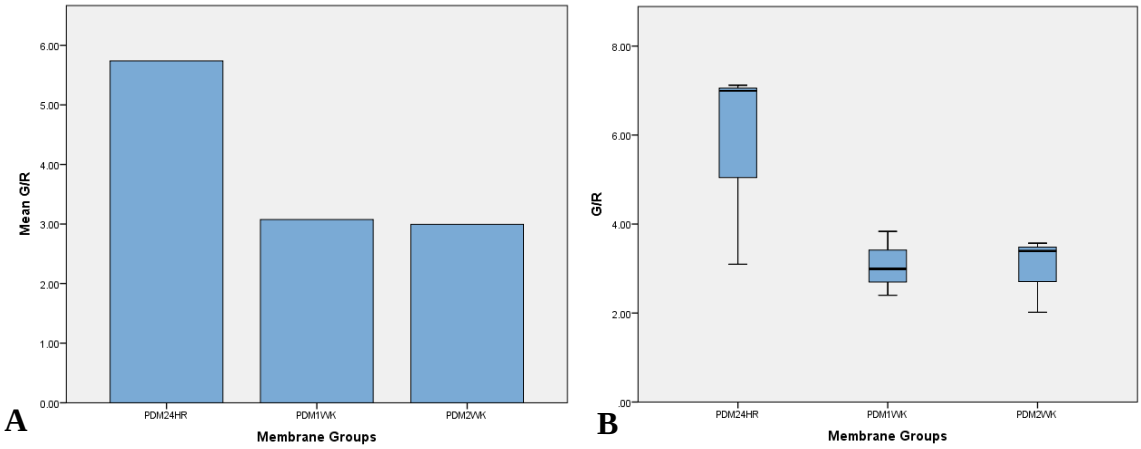

Figure 3-7. Live/dead data for PDM group at each time point. A) Bar graph for mean G/R for live/dead assay for each time point for PDM group B) Box plot for G/R values for live/dead assay for each time point for PDM groups.

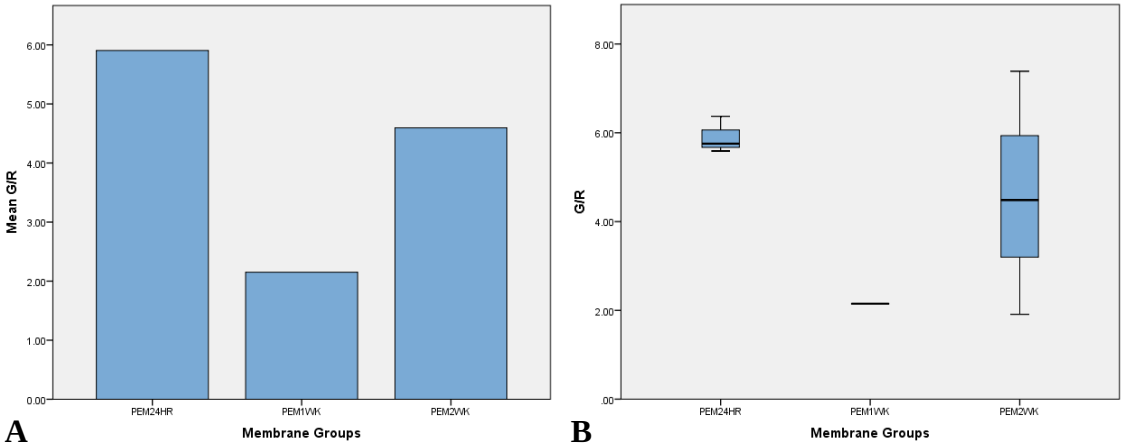

Figure 3-8. Live/dead data for PEM group at each time point. A) Bar graph for mean G/R for live/dead assay for each time point for PEM group**,** B) Box plot for G/R values for live/dead assay for each time point for PEM group.

	ADM 24 HR	***ADM 1 WK***	***ADM 2 WK***	***PDM 24 HR***	***PDM 1 WK***	***PDM 2 WK***	***PEM 24 HR***	***PEM 1 WK***	***PEM 2 WK***
ADM 24HR	--------	*0.050*	*0.050*	*0.827*	--------	--------	*0.513*	--------	--------
ADM 1 WK	*0.050*	--------	*0.050*	--------	*0.513*	--------	--------	*0.050*	--------
ADM 2 WK	*0.050*	*0.050*	--------	--------	--------	*0.059*	--------	--------	*0.050*
PDM 24HR	*0.827*	--------	--------	--------	*0.127*	*0.275*	*0.513*	--------	--------
PDM 1 WK	--------	*0.513*	--------	*0.127*	--------	*0.827*	--------	*0.050*	--------
PDM 2 WK	--------	--------	*0.059*	*0.275*	*0.827*	--------	--------	--------	*0.513*
PEM 24HR	*0.513*	--------	--------	*0.513*	--------	--------	--------	*0.050*	*0.513*
PEM 1WK	--------	*0.050*	--------	--------	*0.050*	--------	*0.050*	--------	*0.513*
PEM 2 WK	--------	--------	*0.050*	--------	--------	*0.513*	*0.513*	*0.513*	--------

Table 3-1. P-values from Mann-Whitney U comparisons for inter-group and intra-group differences for individual time points $\alpha < 0.0056$.

	ADM	***PDM***	***PEM***
ADM	----------	*0.354*	----------
PDM	*0.825*	----------	*0.965*
PEM	*0.354*	*0.965*	----------

Table 3-2. P-values Mann-Whitney U comparisons for inter-group differences for combined time points $\alpha < 0.0056$.

Gingival Fibroblasts Consume and Remodel All Dermal Matrices to a Smoother Surface

Scanning electron microscopy (SEM) is a common method used to observe cells grown on three-dimensional surfaces. While imaging cannot penetrate the surface, SEM can provide useful information regarding characteristics and topography of the matrix, as well as cell interaction on the matrix. Sputter coating the matrices with gold also allowed for improved resolution at higher voltage, thus providing more data.

While quantitative analysis was not used in SEM imaging of the matrices, qualitative differences were noted between time points. Unhydrated controls (Figure 3-9 A-C) appeared to have a compact and compressed matrix among all groups while their hydrated counterparts appeared to be less compressed but with similar surface roughness (Figure 3-9 D-F). At the 24 hour time point (Figure 3-10 D-I), all membranes appeared less rough then the hydrated controls (Figure 3-10 A-C), attributed to initial matrix degradation. By the 1 week time point (Figure 3-11D-I), free strands of broken collagen were noted, with all three groups exhibiting smoother appearing topography compared to the hydrated controls (Figure 3-11 A-C). At the 2 week time point (Figure 3-12 D-I), continued remodeling of the matrix was noted, again apparent by a further decrease in surface roughness compared to the hydrated controls (Figure 3-12 A-C).

While fibroblasts were difficult to visualize within the matrix, the apparent changes in the matrix surfaces can be attributed to fibroblasts remodeling and *de novo* synthesis of new collagen.[103] Given that all the matrices are composed of type I collagen, it is not surprising that all matrices remodeled in a similar fashion.

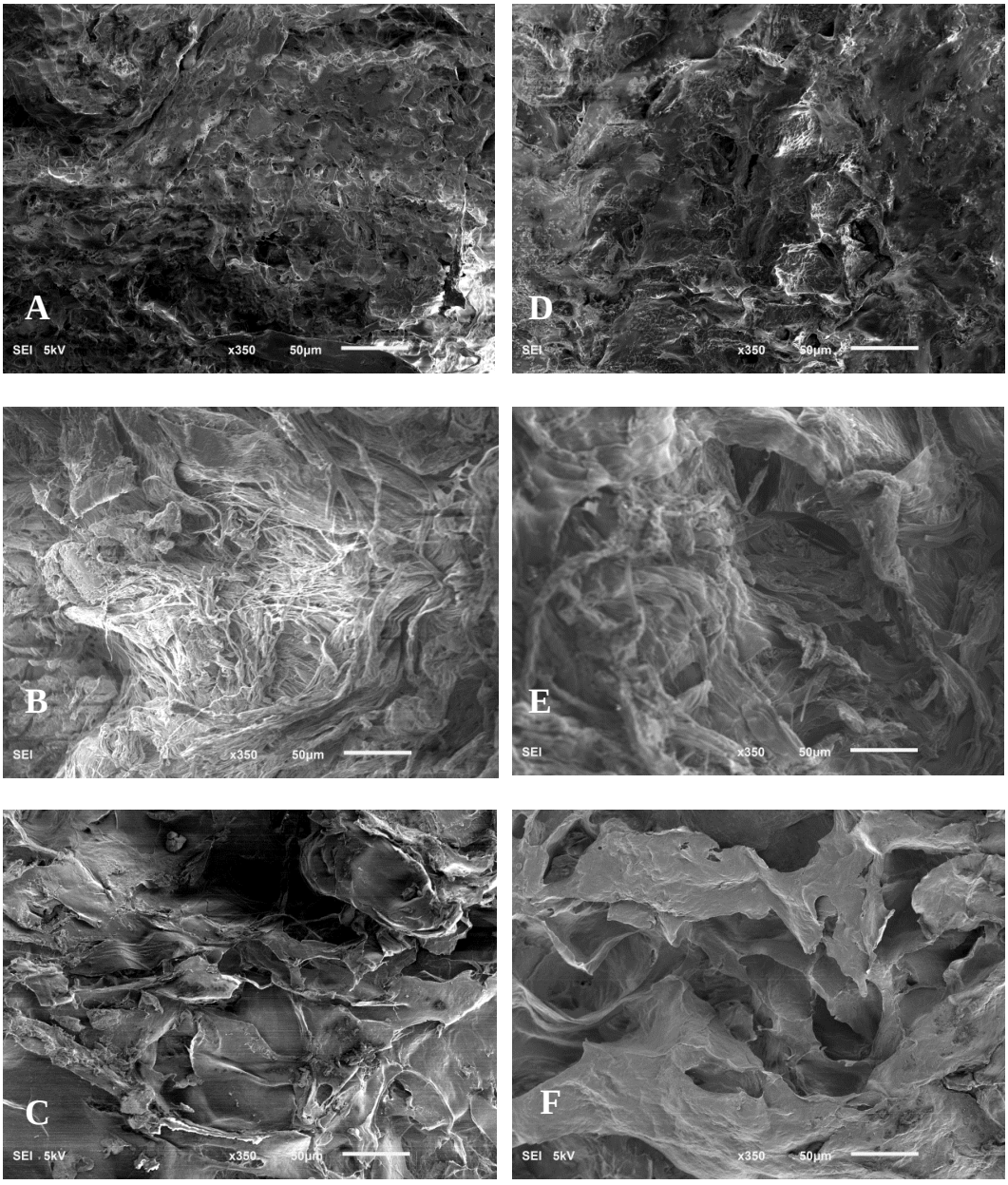

Figure 3-9. SEM for control membranes. Unhydrated membranes at 350x A) ADM, B) PDM, C) PEM; hydrated membranes at 350x D) ADM, E) PDM, F) PEM.

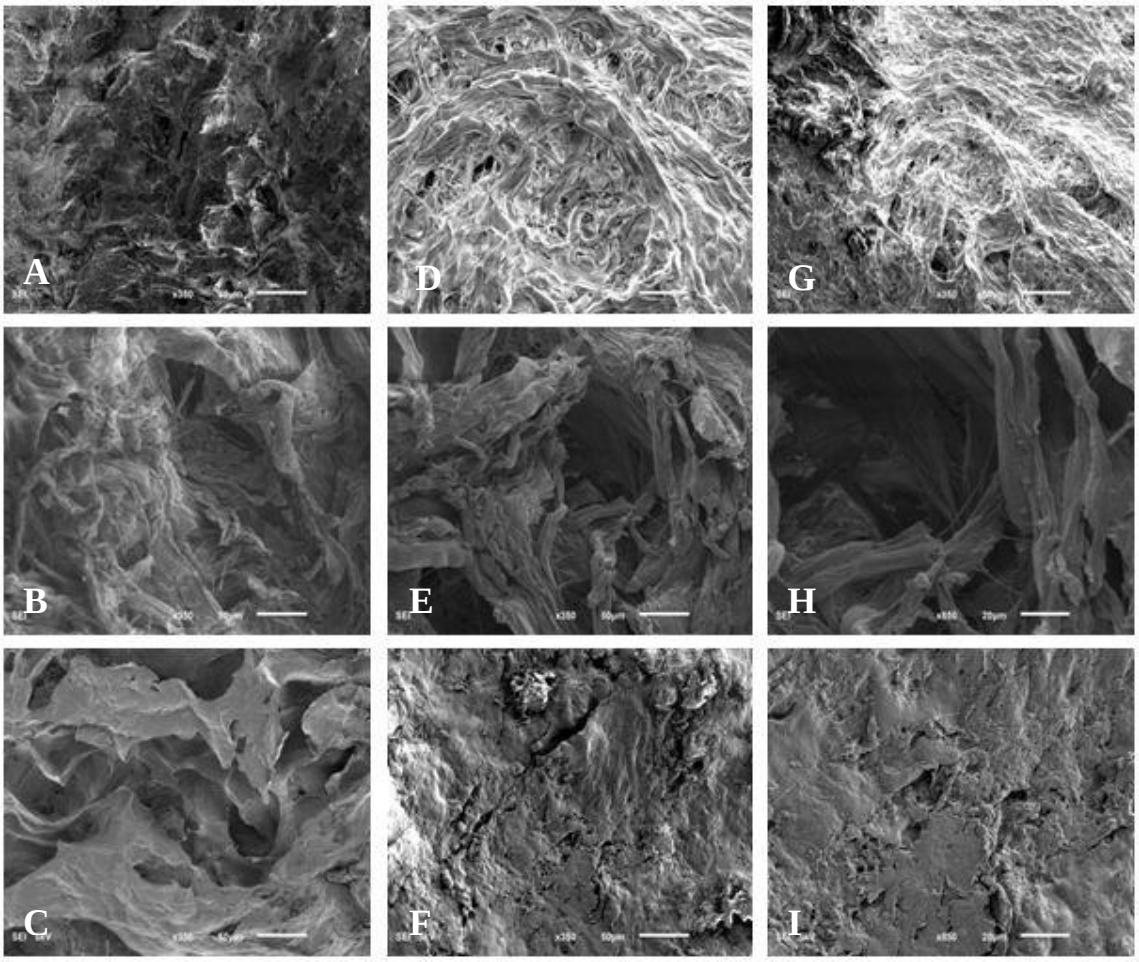

Figure 3-10. SEM for hydrated controls compared to membranes at 24 hours. Hydrated control at 350x A) ADM, B) PDM, C) PEM; 24 hour time points at 350x D) ADM, E) PDM, F) PEM , and 850x G) ADM, H) PDM, I) PEM.

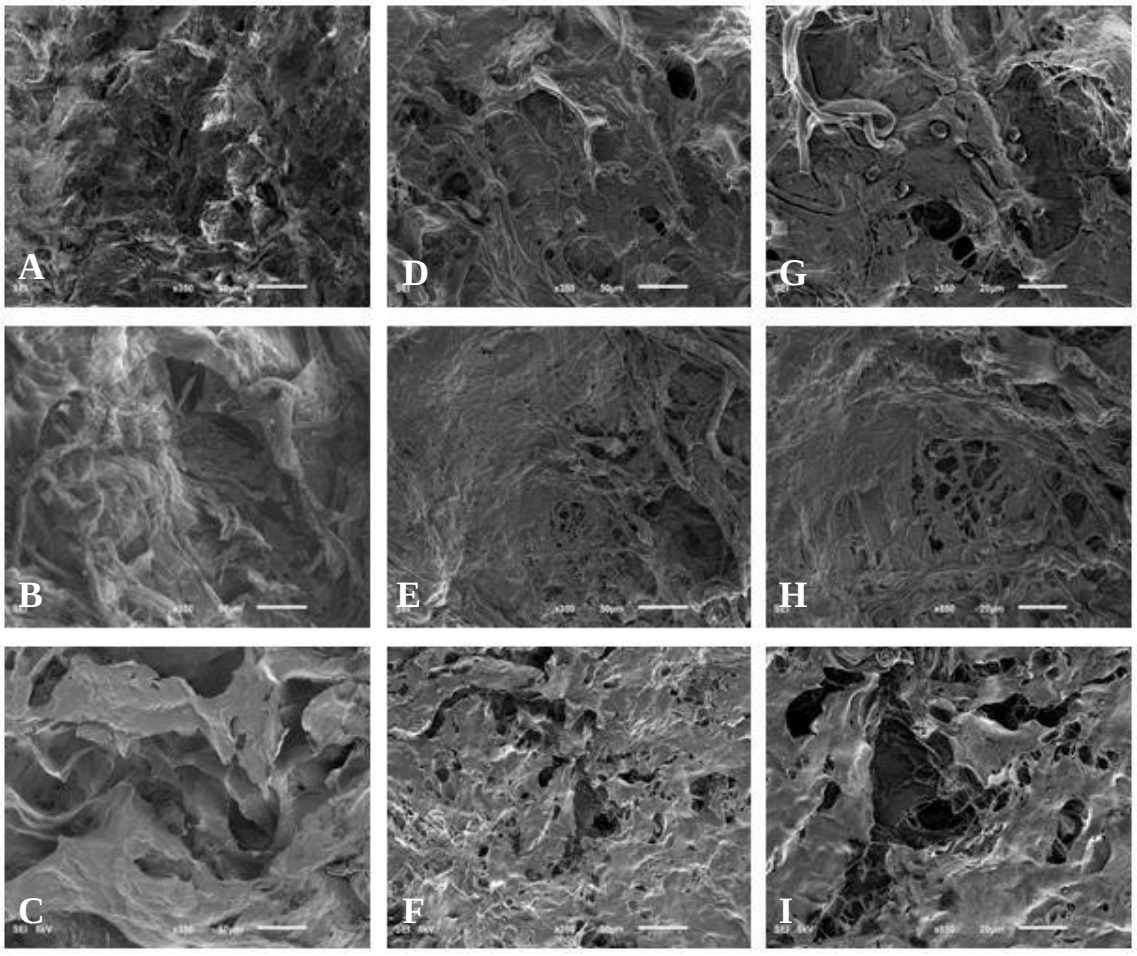

Figure 3-11. SEM for hydrated controls compared to membranes at 1 week. Hydrated control at 350x A) ADM, B) PDM, C) PEM; 1 week time points at 350x D) ADM, E) PDM, F) PEM , and 850x G) ADM, H) PDM, I) PEM.

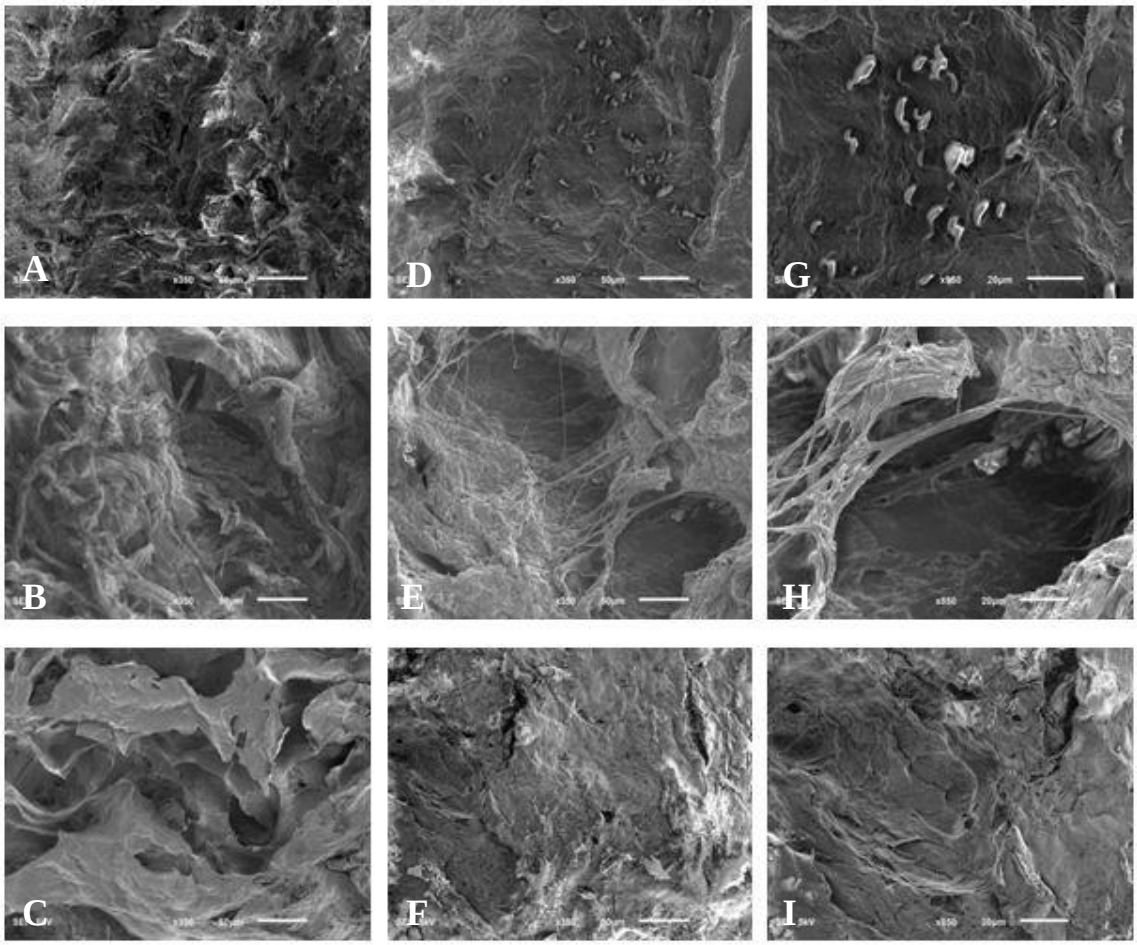

Figure 3-12. SEM for hydrated controls compared to membranes at 2 weeks. Hydrated control at 350x A) ADM, B) PDM, C) PEM; 2 week time points at 350x D) ADM, E) PDM, F) PEM , and 850x G) ADM, H) PDM, I) PEM.

Gingival Fibroblasts Spread Throughout the Full Thickness of the Dermal Matrices

The best section from each matrix at each time point was photographed and assessed. Hematoxylin is basophilic and stained the fibroblast nuclei blue, while the eosin is acidophilic and stained the collagen and extracellular matrix pink. This allowed for easy visualization of the nuclei within the various levels of the matrix.

The basement membrane of the matrices was oriented to the left in all histologic images. While cell count was not performed, fibroblast presence and distribution throughout the three matrices was noted. Fibroblasts were visualized at both 15x and 40x for the majority of membranes at all time points. At 24 hours (Figure 3-13), fibroblasts were seen throughout the full thickness of the matrix for both the ADM (Figure 3-13 A, B) and PEM (Figure 3-13 E, F) groups. No fibroblasts were noted for the PDM group (Figure 3-13 C, D). At 1 week (Figure 3-14), fibroblasts were visualized throughout the various layers of the matrix for both the ADM (Figure 3-14 A, B) and PDM (Figure 3-14 C, D) groups. However, the distribution of fibroblasts was sparse for the PEM group (Figure 3-14 E, F). At 2 weeks (Figure 3-15), fibroblasts were evident throughout the full thickness of the matrix for all three membrane groups (Figure 3-15 A-F).

Based on qualitative inspection alone, ADM was the only group that displayed fibroblasts at all three time points. However all membranes did have fibroblast infiltration through the full-thickness of the matrix at least at one time point.

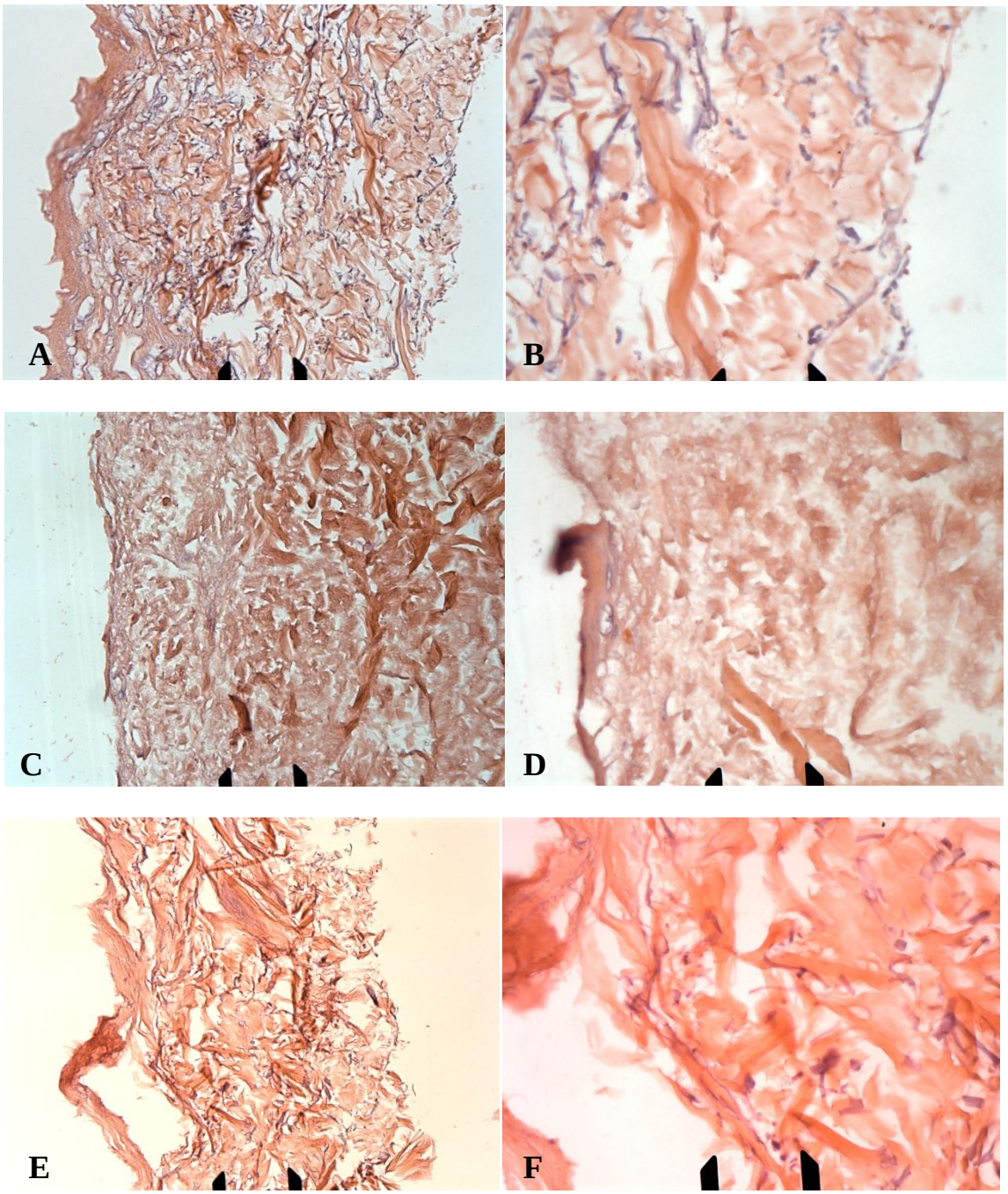

Figure 3-13. H&E for 24 hour time points. A) ADM 15x, B) ADM 40x, C) PDM 15x, D) PDM 40x, E) PEM 15x, F) PEM 40x.

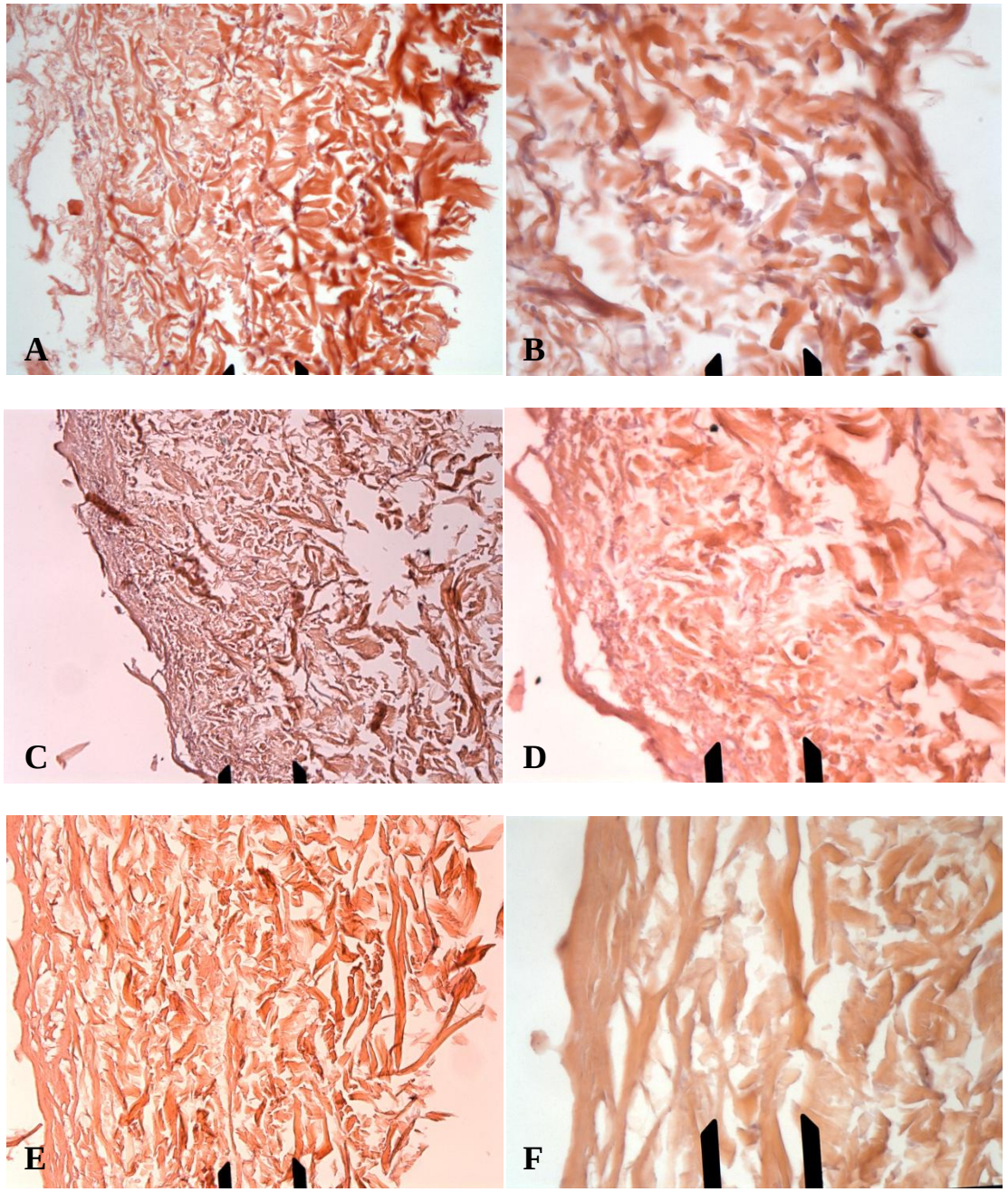

Figure 3-14. H&E for 1 week time points. A) ADM 15x, B) ADM 40x, C) PDM 15x, D) PDM 40x, E) PEM 15x, F) PEM 40x.

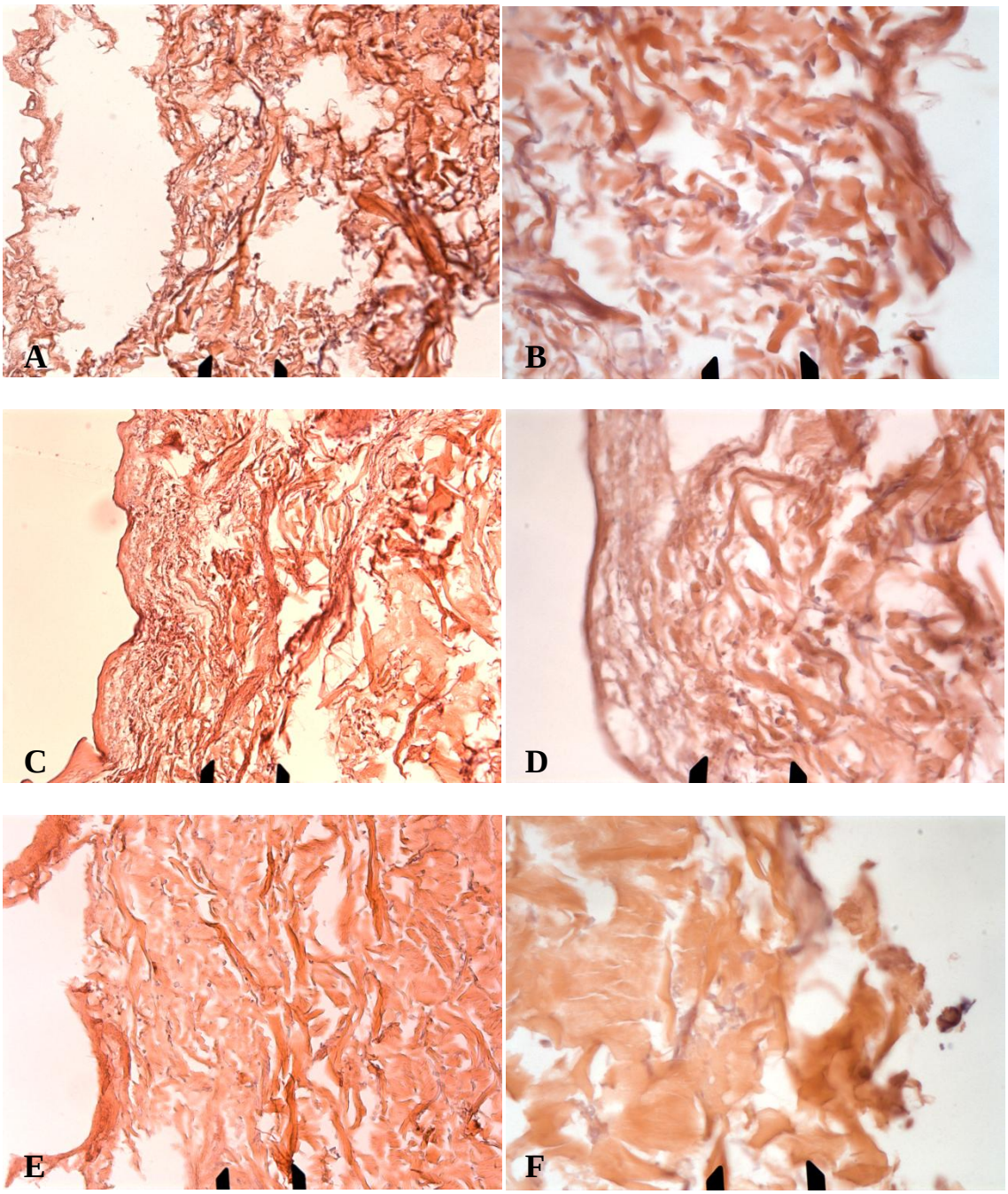

Figure 3-15. H&E for 2 week time points. A) ADM 15x, B) ADM 40x, C) PDM 15x, D) PDM 40x, E) PEM 15x, F) PEM 40x.

CHAPTER IV

DISCUSSION

Previous studies have examined gingival fibroblast viability *in vitro* on ADM allografts. [102, 107, 108] Hakki studied human gingival fibroblast viability using an MTT [(3-(4,5-dimethylthiazol-2-yl)-2,5-diphenyl-tetrazo-lium-bromid)] colorimetric assay, and found that fibroblast viability increased from 5 days to 10 days post-seeding, in conjunction with an increase in cell number. [102] Rodrigues evaluated human gingival fibroblast viability on ADM allografts using flow cytometry, noting a decrease from 96.4% to 94.9%, from day 14 to day 21, respectively.[107] Maia utilized an MTT assay to measure viability of human gingival fibroblast, canine gingival fibroblast, and murine melanoma cell lines grown on ADM allografts.[108] He noted and increase in viability from day 7 to day 14 day, with significantly greater viability at both time points for the human gingival fibroblasts, compared to the canine and murine cell lines.

In this study, confocal imaging was used to visualize live/dead assay results. The ratio of green to red (G/R) pixels was calculated for each membrane and compared within and between groups. Thus, it is difficult to compare values to previous studies utilizing different methods. No significant differences were noted in regards to viability as represented by G/R ratios within and between groups at the 24 hour, 1 week, and 2 week time points (Table 3-1). Negative trends were noted in the ADM and PDM groups, with cell viability decreasing from the 24 hour to the 2 week time point (Figures 3-6 A, 3-7 A). While fibroblast viability in the PEM group decreased from 24 hours to 1 week,

and increased from 1 week to 2 weeks (Figure 3-8 A). It is possible that viability decreased as a function of time due to the matrices becoming overpopulated or confluent, leading to a scarcity of nutrients and build-up of cellular waste, resulting in apoptosis. Likewise, it is possible that viability decreased over time due to the time lapse from when the membranes were removed from culture to when they were analyzed. In addition, is possible that the cellular viability across all groups was decreased in this study due to a cross-species interaction between rat fibroblasts grown on human dermis.

Cellular distribution of fibroblasts on ADM allografts has been reported at various portions of the matrix at different time points.[107, 108] Rodrigues noted that fibroblasts were adherent and unevenly distributed across the surface of the matrix at 7 days. By 14 days the fibroblasts formed a confluent monolayer, with a higher proportion of cells noted on the inner aspect of the matrix when cross sections were taken from the border, compared to central slices.[107] Maia noted similar results with human gingival fibroblasts, again observing that few fibroblasts were present on the interior of the ADM allograft.[108] Canine fibroblasts in that same studied failed to reach confluence on the surface and appeared unevenly distributed at 7 days and 14 days.

In this study, rat gingival fibroblasts were observed at various levels within the matrix. Fibroblasts were seeded on the dermal aspect, but nuclei could be observed near the basement membrane portion of the matrix. Histologic specimens at 24 hours (Figure 3-13) showed fibroblasts dispersed throughout the full thickness of the matrix for both the ADM and PEM groups (Figure A, B, E, F), but were not discernible in the PDM group (Figure 3-13 C, D). At 1 week (Figure 3-14), fibroblasts were seen throughout the

various layers of the matrix for both the ADM and PDM groups (Figure 3-14 A, B, C, D). However, the distribution of fibroblasts was sparse for the PEM group (Figure 3-14 E, F). At 2 weeks (Figure 3-15 A-F), fibroblast were evident throughout the full thickness of the matrix for all three membrane groups. Based on qualitative inspection alone, ADM was the only group that displayed fibroblasts at all three time points.

Changes in ADM surface texture following human gingival fibroblasts seeding have been shown via SEM.[102, 103] Hakki noted the establishment of tissue layers arranged in a 3-D network consisting of fibroblasts, new collagen, and native matrix, with extra-cellular matrix production significantly increasing from 14 to 28 days.[102] In this study, surface roughness decreased as time progressed for each membrane examined. Even though fibroblasts were difficult to individually visualize within the matrix, the apparent changes in the matrix topography can most likely be attributed to fibroblasts remodeling and *de novo* synthesis of new collagen.

Future research in this topic should be aimed at *in vivo* implantation of these matrices. A canine model would be ideal for intra-oral application, with coronal advancement of existing tissue over the graft. Histologic comparison at various time points could then be used to visualize matrix degradation and incorporation into the native tissue.

CHAPTER V

CONCLUSION

All three dermal matrices demonstrated that they could support rat gingival fibroblast growth. There were no apparent differences in cell viability or cell distribution based on the live/dead assay and H&E sections. Matrix degradation and remodeling also appeared similar for all three groups visualized via SEM. All three products are commercially available, and as such have amassed a clinical track record in the dental market. Given the results of the study, other factors such as price, handling characteristics, and hydration time seem more relevant to the clinician when deciding which product to choose for surgical correction of root coverage.

REFERENCES

1. Newman MG, Takei, H.H., Klokkevold, P.R., Carranza, F.M. Carranza's Clinical Periodontology. 11 ed. 2012. St. Louis, Missouri: Elsever Saunders.
2. American Academy of Periodontology. Glossary of Periodontal Terms. American Academy of Periodontology. Chicago; 2001.
3. Armitage GC. Development of a classification system for periodontal diseases and conditions. Ann Periodontol 1999;4(1):1-6.
4. Armitage GC. Periodontal diagnoses and classification of periodontal diseases. Periodontol 2000 2004;34:9-21.
5. Goldstein M, Brayer L, Schwartz Z. A critical evaluation of methods for root coverage. Crit Rev Oral Biol Med 1996;7(1):87-98.
6. Page RC, Schroeder HE. Pathogenesis of inflammatory periodontal disease. A summary of current work. Lab Invest 1976;34(3):235-49.
7. Socransky SS, Haffajee AD. Microbial mechanisms in the pathogenesis of destructive periodontal diseases: a critical assessment. J Periodontal Res 1991;26(3 Pt 2):195-212.
8. Baker DL, Seymour GJ. The possible pathogenesis of gingival recession. A histological study of induced recession in the rat. J Clin Periodontol 1976;3(4):208-19.
9. Smith RG. Gingival recession. Reappraisal of an enigmatic condition and a new index for monitoring. J Clin Periodontol 1997;24(3):201-5.

10. Breitenmoser J, Mormann W, Muhlemann HR. Damaging effects of toothbrush bristle end form on gingiva. J Periodontol 1979;50(4):212-6.
11. Smukler H, Landsberg J. The toothbrush and gingival traumatic injury. J Periodontol 1984;55(12):713-9.
12. Pini Prato G. Mucogingival deformities. Ann Periodontol 1999;4(1):98-101.
13. Periodontology AAo. Tobacco use and the periodontal patient. J Periodontol 1996;67(1):51-6.
14. Monten U, Wennstrom JL, Ramberg P. Periodontal conditions in male adolescents using smokeless tobacco (moist snuff). J Clin Periodontol 2006;33(12):863-8.
15. Kotansky K, Goldberg M, Tenenbaum HC, Mock D. Factitious injury of the oral mucosa: a case series. J Periodontol 1995;66(3):241-5.
16. Johnson CD, Matt MK, Dennison D, Brown RS, Koh S. Preventing factitious gingival injury in an autistic patient. J Am Dent Assoc 1996;127(2):244-7.
17. Batenhorst KF, Bowers GM, Williams JE, Jr. Tissue changes resulting from facial tipping and extrusion of incisors in monkeys. J Periodontol 1974;45(9):660-8.
18. Steiner GG, Pearson JK, Ainamo J. Changes of the marginal periodontium as a result of labial tooth movement in monkeys. J Periodontol 1981;52(6):314-20.
19. Nunn ME, Harrel SK. The effect of occlusal discrepancies on periodontitis. I. Relationship of initial occlusal discrepancies to initial clinical parameters. J Periodontol 2001;72(4):485-94.

20. Harrel SK, Nunn ME. The effect of occlusal discrepancies on periodontitis. II. Relationship of occlusal treatment to the progression of periodontal disease. J Periodontol 2001;72(4):495-505.

21. Dorfman HS. Mucogingival changes resulting from mandibular incisor tooth movement. Am J Orthod 1978;74(3):286-97.

22. Coatoam GW, Behrents RG, Bissada NF. The width of keratinized gingiva during orthodontic treatment: its significance and impact on periodontal status. J Periodontol 1981;52(6):307-13.

23. Donaldson D. Gingival recession associated with temporary crowns. J Periodontol 1973;44(11):691-6.

24. Gartrell JR, Mathews DP. Gingival recession. The condition, process, and treatment. Dent Clin North Am 1976;20(1):199-213.

25. Lang NP, Loe H. The relationship between the width of keratinized gingiva and gingival health. J Periodontol 1972;43(10):623-7.

26. Miyasato M, Crigger M, Egelberg J. Gingival condition in areas of minimal and appreciable width of keratinized gingiva. J Clin Periodontol 1977;4(3):200-9.

27. Dorfman HS, Kennedy JE, Bird WC. Longitudinal evaluation of free autogenous gingival grafts. J Clin Periodontol 1980;7(4):316-24.

28. Kennedy JE, Bird WC, Palcanis KG, Dorfman HS. A longitudinal evaluation of varying widths of attached gingiva. J Clin Periodontol 1985;12(8):667-75.

29. Stoner JE, Mazdyasna S. Gingival recession in the lower incisor region of 15-year-old subjects. J Periodontol 1980;51(2):74-6.

30. Sullivan HC, Atkins JH. Free autogenous gingival grafts. I. Principles of successful grafting. Periodontics 1968;6(3):121-9.

31. Sullivan HC, Atkins JH. Free autogenous gingival grafts. 3. Utilization of grafts in the treatment of gingival recession. Periodontics 1968;6(4):152-60.

32. Miller PD, Jr. A classification of marginal tissue recession. Int J Periodontics Restorative Dent 1985;5(2):8-13.

33. Loe H, Anerud A, Boysen H. The natural history of periodontal disease in man: prevalence, severity, and extent of gingival recession. J Periodontol 1992;63(6):489-95.

34. Serino G, Wennstrom JL, Lindhe J, Eneroth L. The prevalence and distribution of gingival recession in subjects with a high standard of oral hygiene. J Clin Periodontol 1994;21(1):57-63.

35. Albandar JM, Kingman A. Gingival recession, gingival bleeding, and dental calculus in adults 30 years of age and older in the United States, 1988-1994. J Periodontol 1999;70(1):30-43.

36. Albandar JM, Brunelle JA, Kingman A. Destructive periodontal disease in adults 30 years of age and older in the United States, 1988-1994. J Periodontol 1999;70(1):13-29.

37. Beck JD, Drake CW. Do root lesions tend to develop in the same people who develop coronal lesions? J Public Health Dent 1997;57(2):82-8.

38. Pfeifer JS, Heller R. Histologic evaluation of full and partial thickness lateral repositioned flaps: a pilot study. J Periodontol 1971;42(6):331-3.

39. Grupe HE WR. Repair of gingival defects by a sliding flap operation. Journal of Periodontology 1956;27(2):4.

40. Cohen DW, Ross SE. The double papillae repositioned flap in periodontal therapy. J Periodontol 1968;39(2):65-70.

41. Miller PD, Jr. Root coverage using a free soft tissue autograft following citric acid application. Part 1: Technique. Int J Periodontics Restorative Dent 1982;2(1):65-70.

42. Holbrook T, Ochsenbein C. Complete coverage of the denuded root surface with a one-stage gingival graft. Int J Periodontics Restorative Dent 1983;3(3):8-27.

43. Allen EP, Miller PD, Jr. Coronal positioning of existing gingiva: short term results in the treatment of shallow marginal tissue recession. J Periodontol 1989;60(6):316-9.

44. Tarnow DP. Semilunar coronally repositioned flap. J Clin Periodontol 1986;13(3):182-5.

45. Maynard JG, Jr. Coronal positioning of a previously placed autogenous gingival graft. J Periodontol 1977;48(3):151-5.

46. Bernimoulin JP, Luscher B, Muhlemann HR. Coronally repositioned periodontal flap. Clinical evaluation after one year. J Clin Periodontol 1975;2(1):1-13.

47. Langer B, Langer L. Subepithelial connective tissue graft technique for root coverage. J Periodontol 1985;56(12):715-20.

48. Tinti C, Vincenzi G, Cortellini P, Pini Prato G, Clauser C. Guided tissue regeneration in the treatment of human facial recession. A 12-case report. J Periodontol 1992;63(6):554-60.

49. Prato GP, Clauser C, Magnani C, Cortellini P. Resorbable membrane in the treatment of human buccal recession: a nine-case report. Int J Periodontics Restorative Dent 1995;15(3):258-67.

50. Roccuzzo M, Lungo M, Corrente G, Gandolfo S. Comparative study of a bioresorbable and a non-resorbable membrane in the treatment of human buccal gingival recessions. J Periodontol 1996;67(1):7-14.

51. Dodge J, Henderson, R., Greenwell, H. . Root Coverage without a palatal donar site, using an acellular dermal graft. Periodontal Insights 1998;5(4):5.

52. Guinard EA, Caffesse RG. Treatment of localized gingival recessions. Part I. Lateral sliding flap. J Periodontol 1978;49(7):351-6.

53. Bjorn H. Free transplantation of gingival propria. Tandlakarforb Tidning 1963;55.

54. Pennel B, and King, K. Free autogenous gingival graft. Annual Meeting of the Philadelphia Society of Periodontology. Pennsylvania; 1964.

55. Nery EB, Davies EE. The historical development of mucogingival surgery. J West Soc Periodontol Periodontal Abstr 1976;24(4):149-61.

56. Tolmie PN, Rubins RP, Buck GS, Vagianos V, Lanz JC. The predictability of root coverage by way of free gingival autografts and citric acid application: an

evaluation by multiple clinicians. Int J Periodontics Restorative Dent 1991;11(4):261-71.

57. Pasquinelli KL. The histology of new attachment utilizing a thick autogenous soft tissue graft in an area of deep recession: a case report. Int J Periodontics Restorative Dent 1995;15(3):248-57.

58. Chambrone L, Chambrone D, Pustiglioni FE, Chambrone LA, Lima LA. Can subepithelial connective tissue grafts be considered the gold standard procedure in the treatment of Miller Class I and II recession-type defects? J Dent 2008;36(9):659-71.

59. Bruno JF. Connective tissue graft technique assuring wide root coverage. Int J Periodontics Restorative Dent 1994;14(2):126-37.

60. Zucchelli G, De Sanctis M. Treatment of multiple recession-type defects in patients with esthetic demands. J Periodontol 2000;71(9):1506-14.

61. Guiha R, el Khodeiry S, Mota L, Caffesse R. Histological evaluation of healing and revascularization of the subepithelial connective tissue graft. J Periodontol 2001;72(4):470-8.

62. Bruno JF, Bowers GM. Histology of a human biopsy section following the placement of a subepithelial connective tissue graft. Int J Periodontics Restorative Dent 2000;20(3):225-31.

63. Harris RJ. Successful root coverage: a human histologic evaluation of a case. Int J Periodontics Restorative Dent 1999;19(5):439-47.

64. Goldstein M, Boyan BD, Cochran DL, Schwartz Z. Human histology of new attachment after root coverage using subepithelial connective tissue graft. J Clin Periodontol 2001;28(7):657-62.

65. Cummings LC, Kaldahl WB, Allen EP. Histologic evaluation of autogenous connective tissue and acellular dermal matrix grafts in humans. J Periodontol 2005;76(2):178-86.

66. Harris RJ. Histologic evaluation of connective tissue grafts in humans. Int J Periodontics Restorative Dent 2003;23(6):575-83.

67. Pini Prato G, Clauser C, Cortellini P, et al. Guided tissue regeneration versus mucogingival surgery in the treatment of human buccal recessions. A 4-year follow-up study. J Periodontol 1996;67(11):1216-23.

68. Harris RJ. GTR for root coverage: a long-term follow-up. Int J Periodontics Restorative Dent 2002;22(1):55-61.

69. Cortellini P, Clauser C, Prato GP. Histologic assessment of new attachment following the treatment of a human buccal recession by means of a guided tissue regeneration procedure. J Periodontol 1993;64(5):387-91.

70. Griffin TJ, Cheung WS, Zavras AI, Damoulis PD. Postoperative complications following gingival augmentation procedures. J Periodontol 2006;77(12):2070-9.

71. Greenwell H, Bissada NF, Henderson RD, Dodge JR. The deceptive nature of root coverage results. J Periodontol 2000;71(8):1327-37.

72. Biohorizons. Alloderm History and Processing; 2012. Retrieved from https://vsr.biohorizons.com/GetDocument?DocumentID=38898.

73. Livesey SA, del Campo AA, Nag A, Nichols KB, Coleman C, inventors. Methods for Processing and Preserving Collagen-Based Tissues for Transplantation. 1994 August 9, 1994.

74. Livesey SA, Herndon DN, Hollyoak MA, Atkinson YH, Nag A. Transplanted acellular allograft dermal matrix. Potential as a template for the reconstruction of viable dermis. Transplantation 1995;60(1):1-9.

75. Holton LH, 3rd, Kim D, Silverman RP, et al. Human acellular dermal matrix for repair of abdominal wall defects: review of clinical experience and experimental data. J Long Term Eff Med Implants 2005;15(5):547-58.

76. Wainwright D, Madden M, Luterman A, et al. Clinical evaluation of an acellular allograft dermal matrix in full-thickness burns. J Burn Care Rehabil 1996;17(2):124-36.

77. Eppley BL. Experimental assessment of the revascularization of acellular human dermis for soft-tissue augmentation. Plast Reconstr Surg 2001;107(3):757-62.

78. Wong AK, Schonmeyr B, Singh P, et al. Histologic analysis of angiogenesis and lymphangiogenesis in acellular human dermis. Plast Reconstr Surg 2008;121(4):1144-52.

79. Biohorizons. Alloderm RTM Instructions for Use; 2011. Retrieved from http://www.lifecell.com/fileadmin/media/files/downloads/Alloderm_IFU_D.pdf.

80. Biohorizons. Alloderm Technique Manual; 2012. Retrieved from http://www.biohorizons.com/documents/ld101.pdf.

81. Gapski R, Parks CA, Wang HL. Acellular dermal matrix for mucogingival surgery: a meta-analysis. J Periodontol 2005;76(11):1814-22.

82. Harris RJ. Root coverage with a connective tissue with partial thickness double pedicle graft and an acellular dermal matrix graft: a clinical and histological evaluation of a case report. J Periodontol 1998;69(11):1305-11.

83. ZimmerDental. Puros Dermis: Features and Benefits; 2014. Retrieved from http://www.zimmerdental.com/Products/Regenerative/rg_puDermisOverView.aspx.

84. Hinton R, Jinnah RH, Johnson C, Warden K, Clarke HJ. A biomechanical analysis of solvent-dehydrated and freeze-dried human fascia lata allografts. A preliminary report. Am J Sports Med 1992;20(5):607-12.

85. ZimmerDental. Puros Dermis Instructions for Use; 2014. http://www.zimmerdental.com/pdf/lib_infoForUse_PurosDermisInstr.pdf.

86. Barker TS, Cueva MA, Rivera-Hidalgo F, et al. A comparative study of root coverage using two different acellular dermal matrix products. J Periodontol 2010;81(11):1596-603.

87. Wang HL, Romanos GE, Geurs NC, et al. Comparison of two differently processed acellular dermal matrix products for root coverage procedures: a prospective, randomized multicenter study. J Periodontol 2014;85(12):1693-701.

88. DentsplyImplants. PerioDerm Quality, Safety, and Reliability; 2009. Retreived from http://www.kimiatebco.com/extra/collagel/kimiateb4.pdf.

89. DentsplyImplants. PerioDerm Instructions For Use; 2011. Retrieved from http://www.mtf.org/documents/PI_-77_Rev_3.pdf.

90. Shin SH, Cueva MA, Kerns DG, et al. A comparative study of root coverage using acellular dermal matrix with and without enamel matrix derivative. J Periodontol 2007;78(3):411-21.

91. Carney CM, Rossmann JA, Kerns DG, et al. A comparative study of root defect coverage using an acellular dermal matrix with and without a recombinant human platelet-derived growth factor. J Periodontol 2012;83(7):893-901.

92. Strom SC M, G. Collagen as substrate for cell-growht and differentiation. Methods Enzymol 1982;82:11.

93. Hu S, Cui D, Yang X, et al. The crucial role of collagen-binding integrins in maintaining the mechanical properties of human scleral fibroblasts-seeded collagen matrix. Mol Vis 2011;17:1334-42.

94. Burridge K, Molony L, Kelly T. Adhesion plaques: sites of transmembrane interaction between the extracellular matrix and the actin cytoskeleton. J Cell Sci Suppl 1987;8:211-29.

95. Turner CE, Glenney JR, Jr., Burridge K. Paxillin: a new vinculin-binding protein present in focal adhesions. J Cell Biol 1990;111(3):1059-68.

96. Abercrombie M, Dunn GA. Adhesions of fibroblasts to substratum during contact inhibition observed by interference reflection microscopy. Exp Cell Res 1975;92(1):57-62.

97. Izzard CS, Lochner LR. Cell-to-substrate contacts in living fibroblasts: an interference reflexion study with an evaluation of the technique. J Cell Sci 1976;21(1):129-59.

98. Chen WT, Singer SJ. Immunoelectron microscopic studies of the sites of cell-substratum and cell-cell contacts in cultured fibroblasts. J Cell Biol 1982;95(1):205-22.

99. Zamir E, Geiger B. Molecular complexity and dynamics of cell-matrix adhesions. J Cell Sci 2001;114(Pt 20):3583-90.

100. Bershadsky AD, Tint IS, Neyfakh AA, Jr., Vasiliev JM. Focal contacts of normal and RSV-transformed quail cells. Hypothesis of the transformation-induced deficient maturation of focal contacts. Exp Cell Res 1985;158(2):433-44.

101. Geiger B, Bershadsky A, Pankov R, Yamada KM. Transmembrane crosstalk between the extracellular matrix--cytoskeleton crosstalk. Nat Rev Mol Cell Biol 2001;2(11):793-805.

102. Hakki SS, Korkusuz P, Purali N, et al. Attachment, proliferation and collagen type I mRNA expression of human gingival fibroblasts on different biodegradable membranes. Connect Tissue Res 2013;54(4-5):260-6.

103. Sachar A, Strom TA, San Miguel S, et al. Cell-matrix and cell-cell interactions of human gingival fibroblasts on three-dimensional nanofibrous gelatin scaffolds. J Tissue Eng Regen Med 2014;8(11):862-73.

104. Singh D, Singh D, Choi SM, et al. Effect of Extracts of Terminalia chebula on Proliferation of Keratinocytes and Fibroblasts Cells: An Alternative Approach for Wound Healing. Evid Based Complement Alternat Med 2014;2014:701656.

105. San Miguel SM, Opperman LA, Allen EP, Zielinski J, Svoboda KK. Antioxidants counteract nicotine and promote migration via RacGTP in oral fibroblast cells. J Periodontol 2010;81(11):1675-90.

106. Abcam. ab114347-Live and Deac Cell Assay Instructions for Use. 2014:14.

107. Rodrigues AZ, Oliveira PT, Novaes AB, Jr., et al. Evaluation of in vitro human gingival fibroblast seeding on acellular dermal matrix. Braz Dent J 2010;21(3):179-89.

108. Maia LP, Novaes AB, Jr., Souza SL, et al. In vitro evaluation of acellular dermal matrix as a three-dimensional scaffold for gingival fibroblasts seeding. J Periodontol 2011;82(2):293-301.